Auroral Plasma Science with ISR

Joshua Semeter, Boston University

Second law of thermodynamics

All spontaneous processes produce an increase in the entropy of the universe.

Nature makes highly organized and coherent phenomena to make this happen efficiently.

Some examples of entropy accelerators

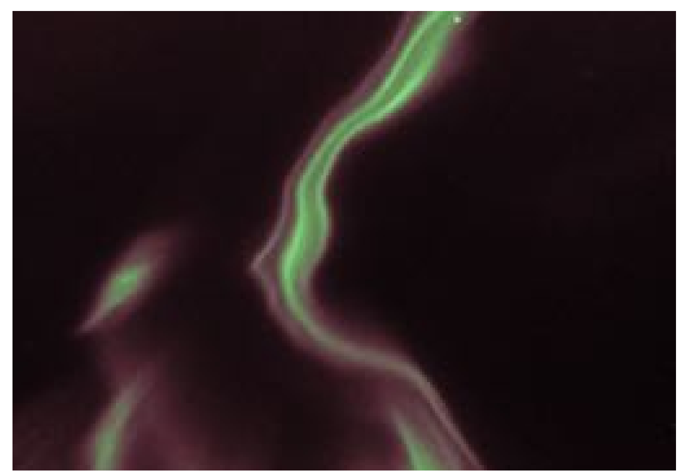

Space Plasmas: Universal Themes

- Emissions illuminate field structure

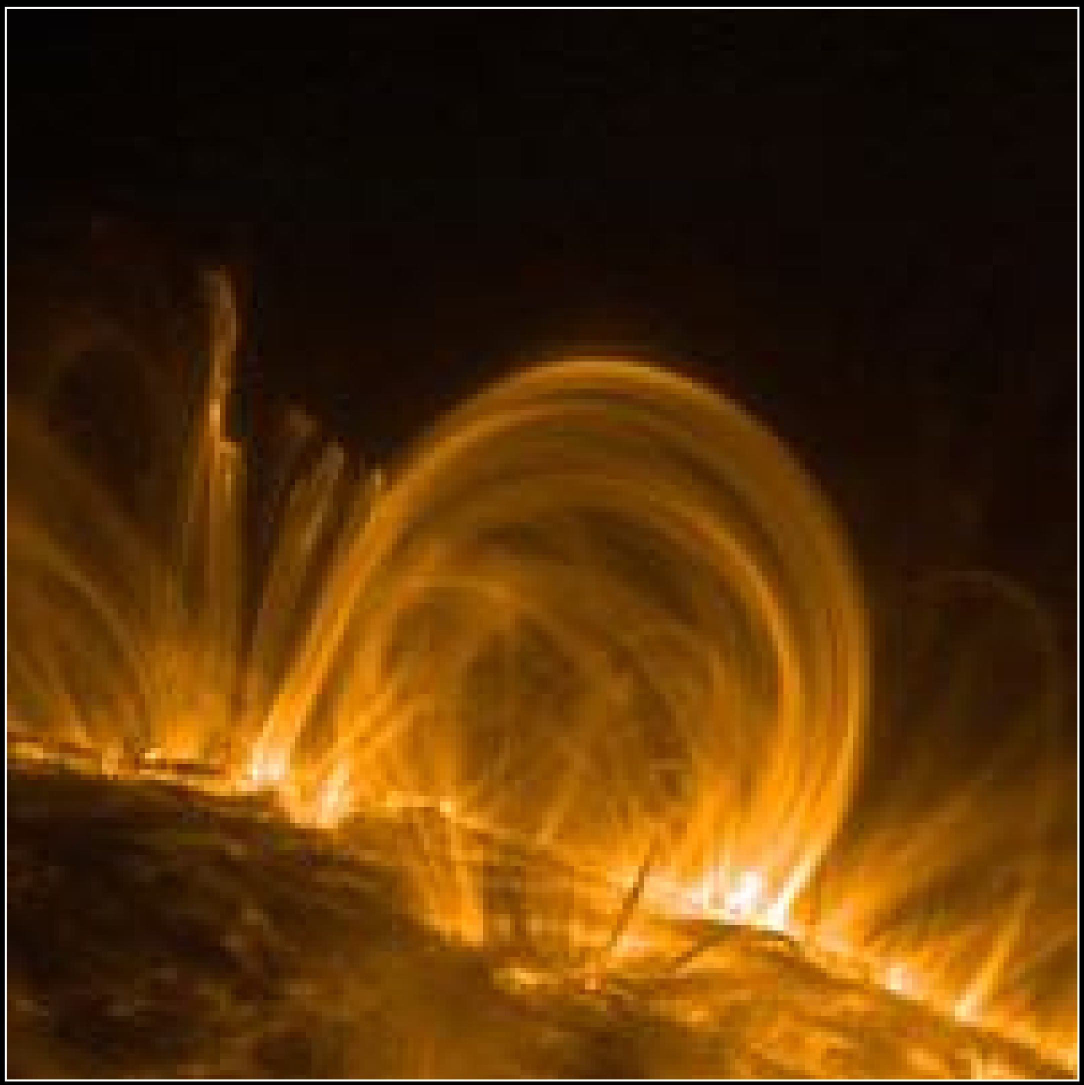

Space Plasmas: Universal Themes

- Emissions illuminate field structure
- Interaction between particles and fields

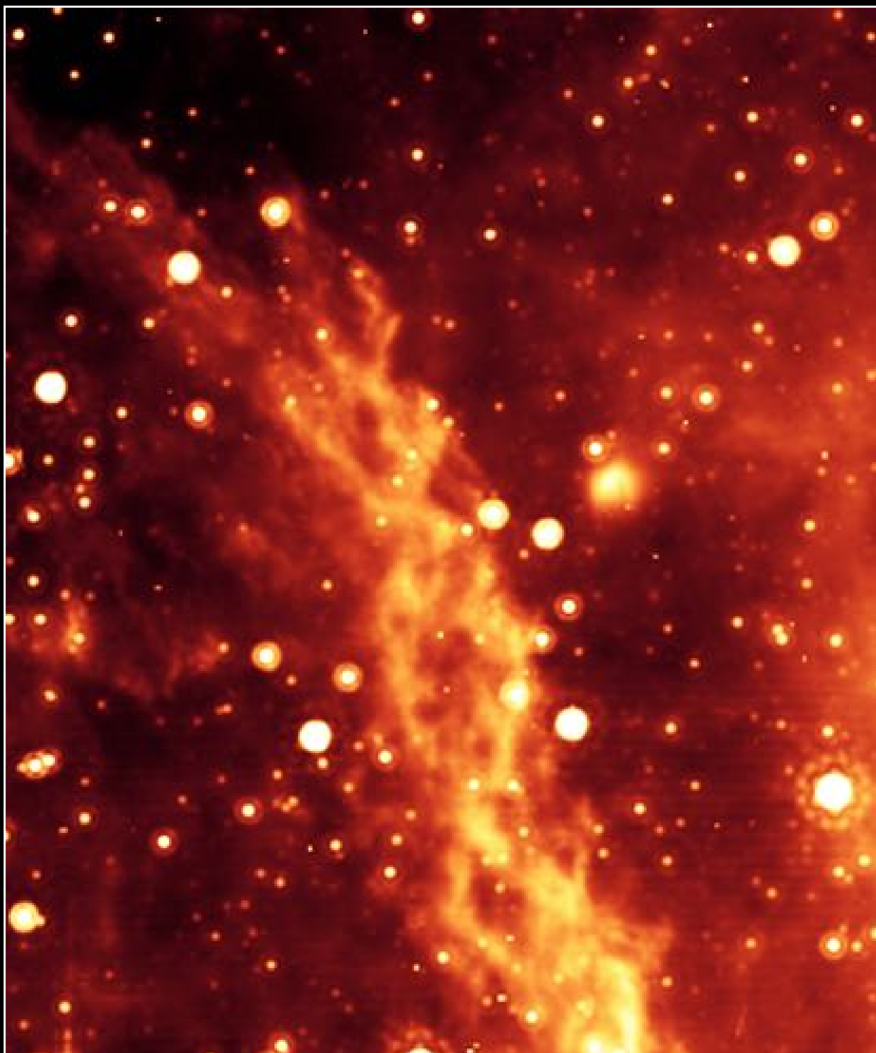

80 light years

15 km

Space Plasmas: Universal Themes

- Emissions illuminate field structure
- Interaction between particles and fields
- Vorticity

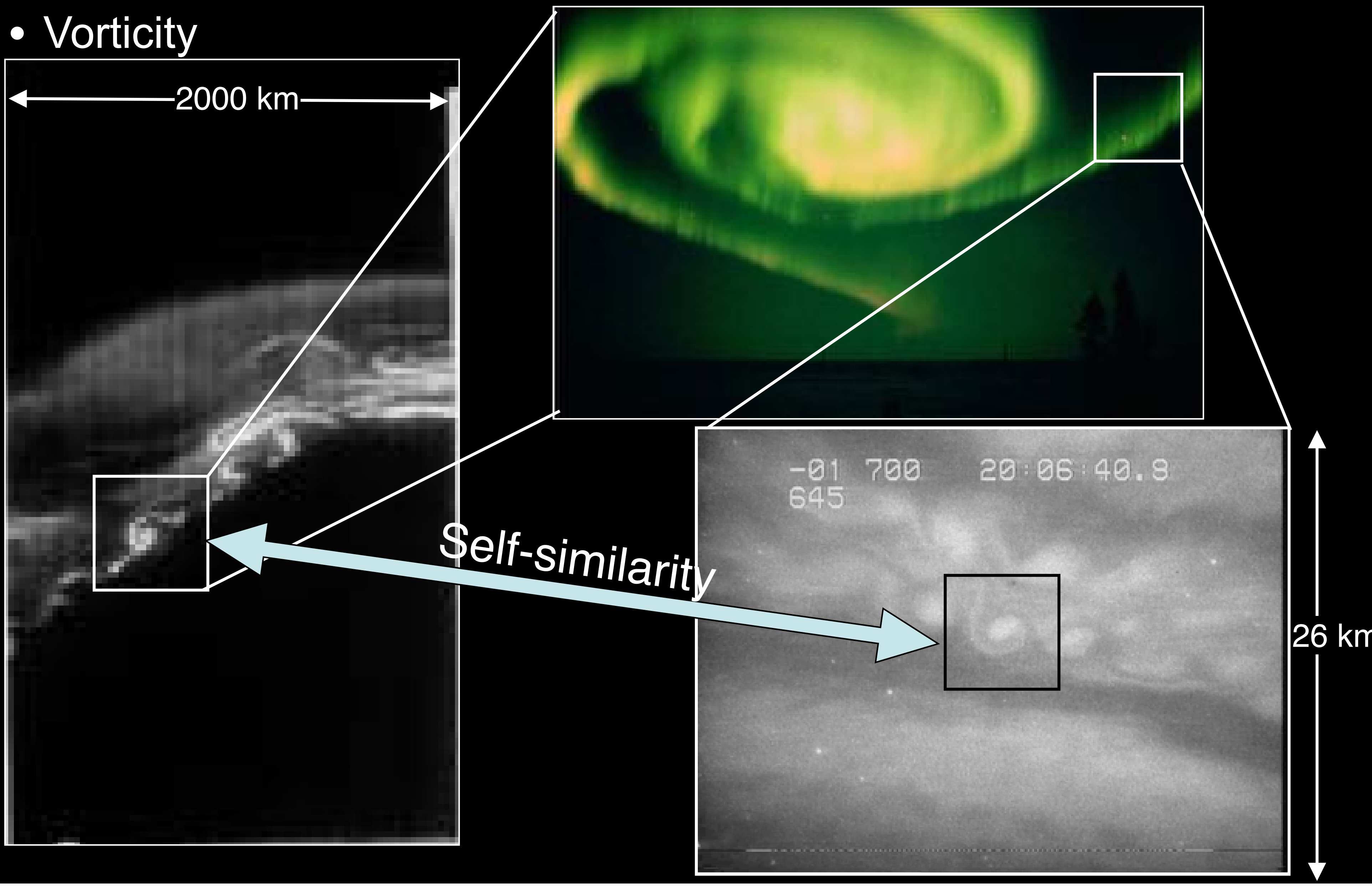

Space Plasmas: Universal Themes

- Emissions illuminate field structure
- Interaction between particles and fields
- Vorticity
- Explosive release of magnetic energy

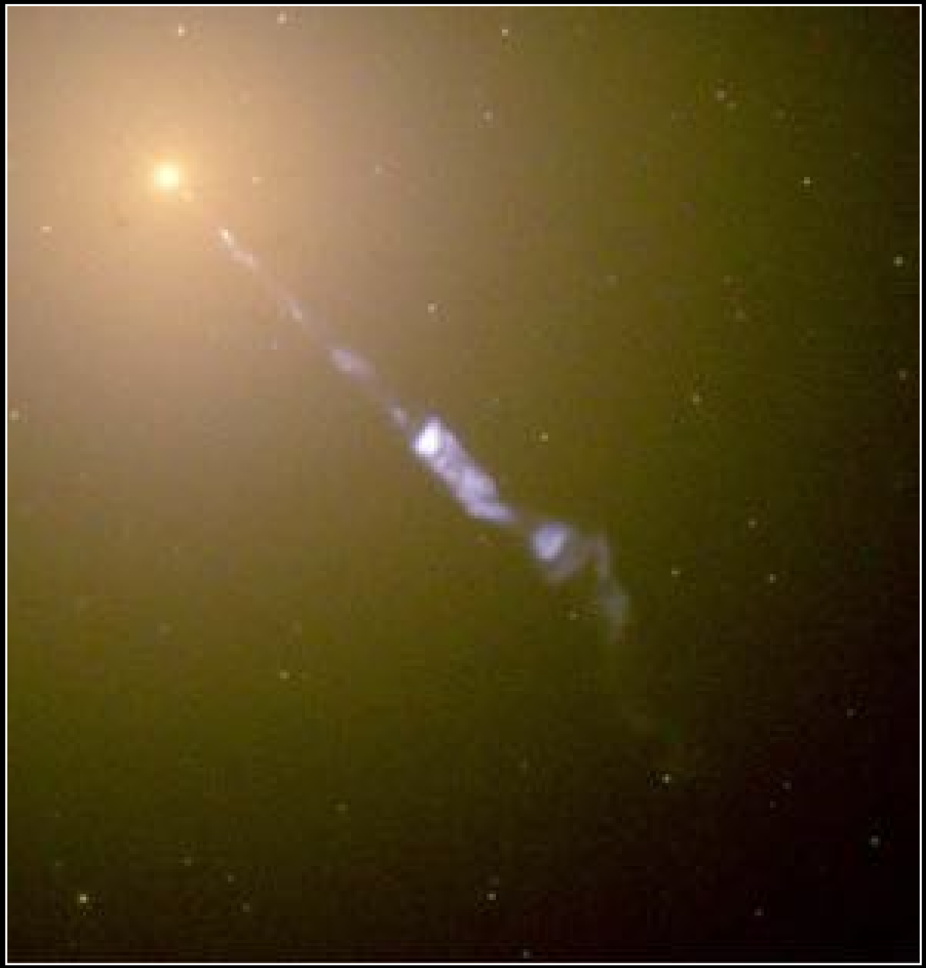

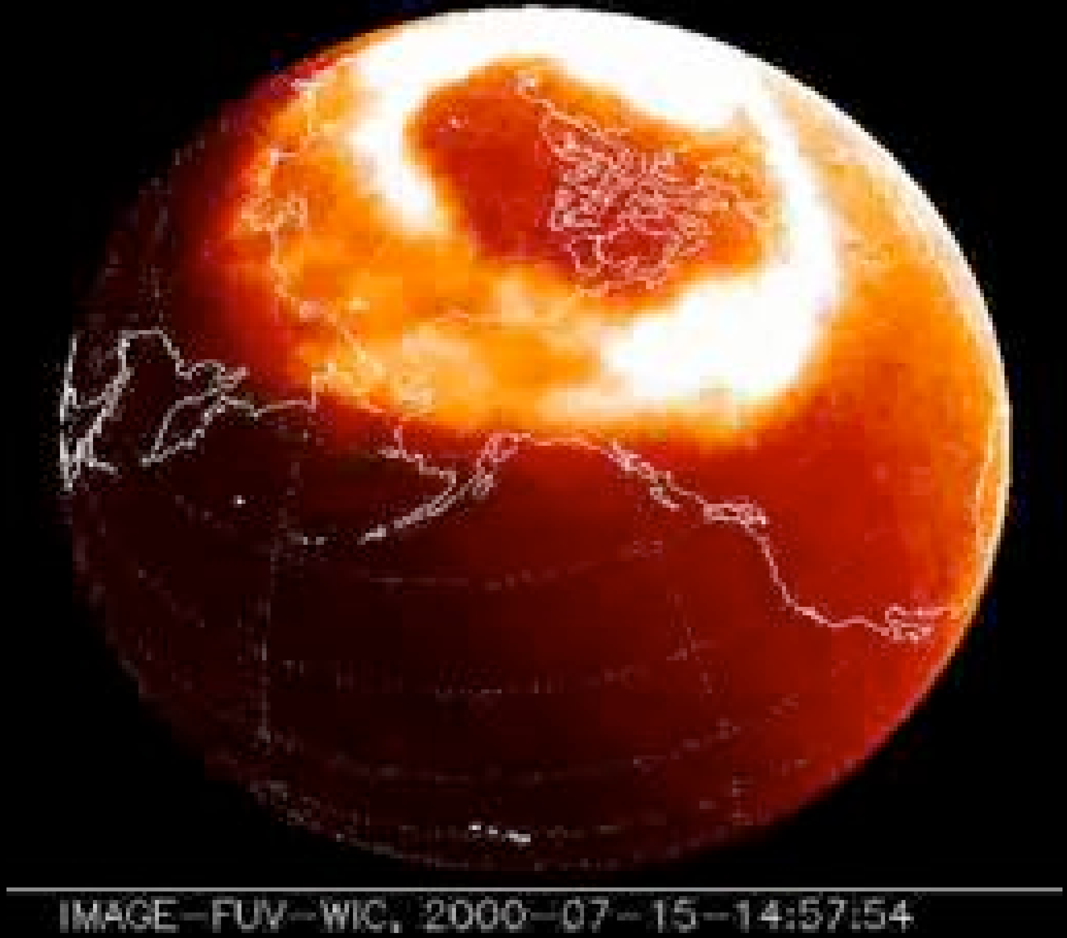

Space Plasmas: Universal Themes

- Emissions illuminate field structure
- Interaction between particles and fields
- Vorticity
- Explosive release of magnetic energy
- Filamentation

Space Plasmas: Universal Themes

- Emissions illuminate field structure
- Interaction between particles and fields
- Vorticity
- Explosive release of magnetic energy
- Filamentation

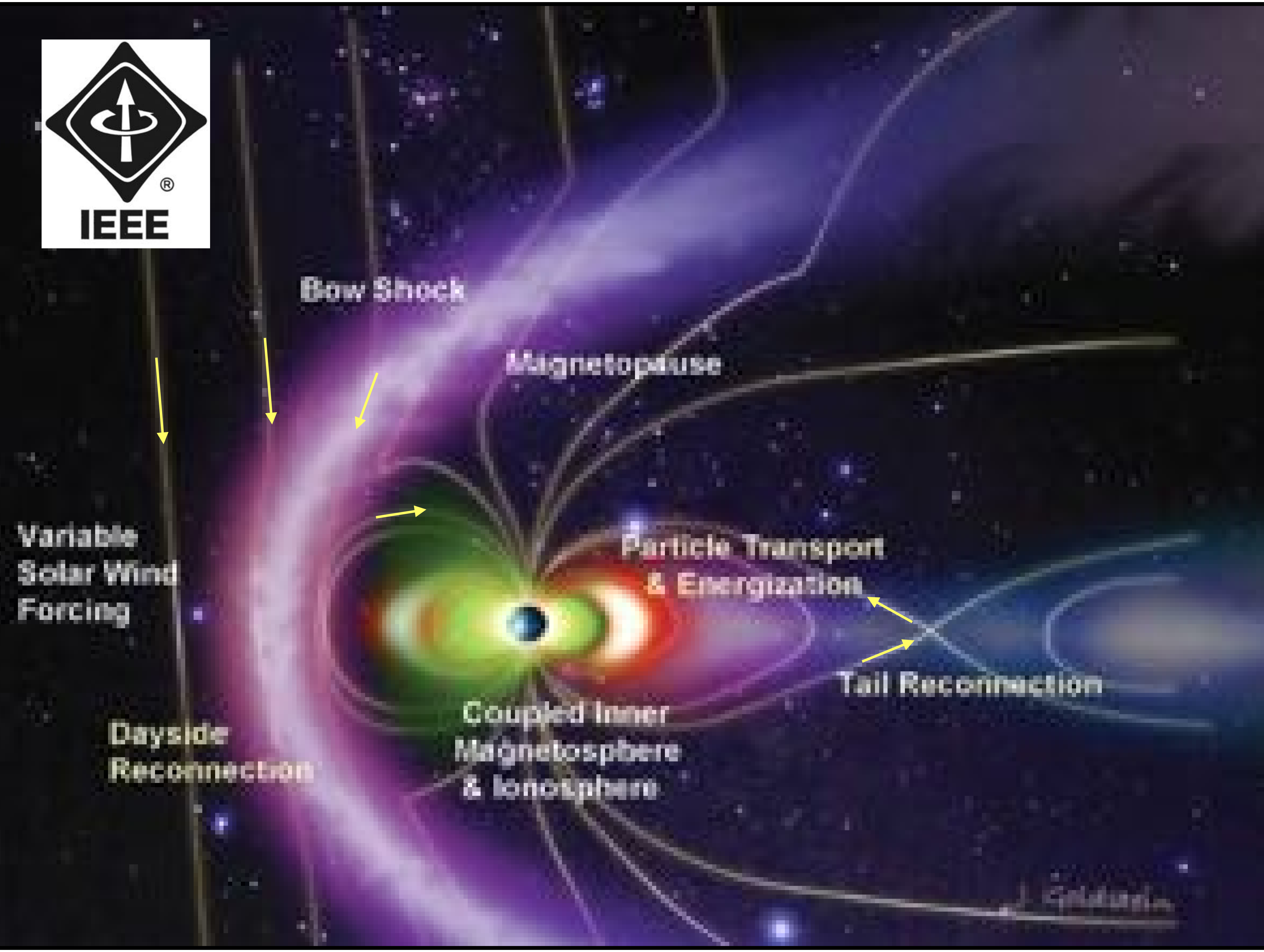
Bow Shock
Magnetopause
Variable
Solar Wind
Forcing
Particle Transport
& Energization
Tail Reconnection
Dayside
Reconnection
Coupled Inner
Magnetosphere
& Ionosphere

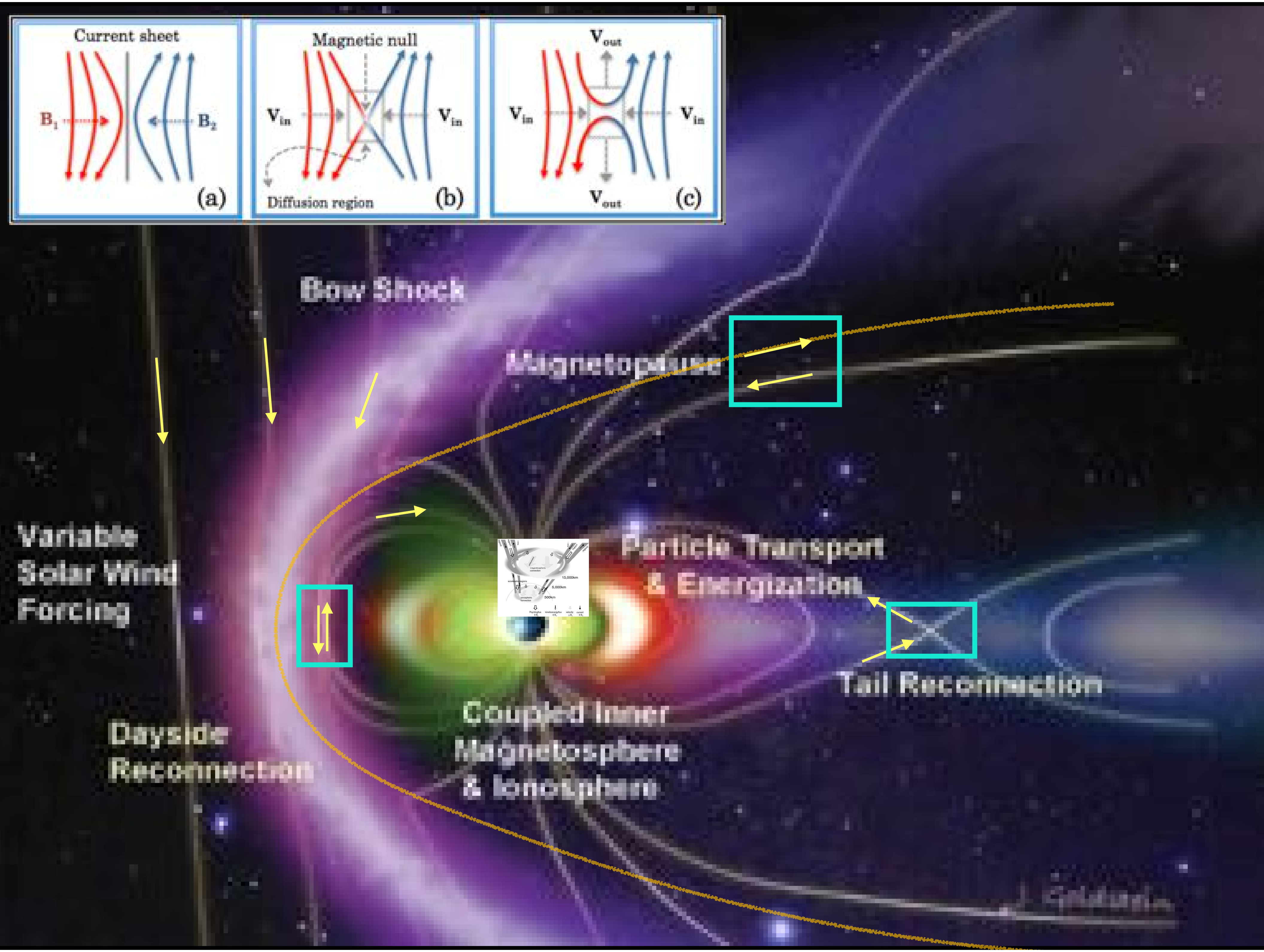

Current sheet
B1
B2
(a)
Magnetic null
Vin
Vin
Diffusion region
(b)
Vout
Vin
Vin
Vout
(c)
Bow Shock
Magnetopause
Variable
Solar Wind
Forcing
Particle Transport
& Energization
Tail Reconnection
Dayside
Reconnection
Coupled Inner
Magnetosphere
& Ionosphere

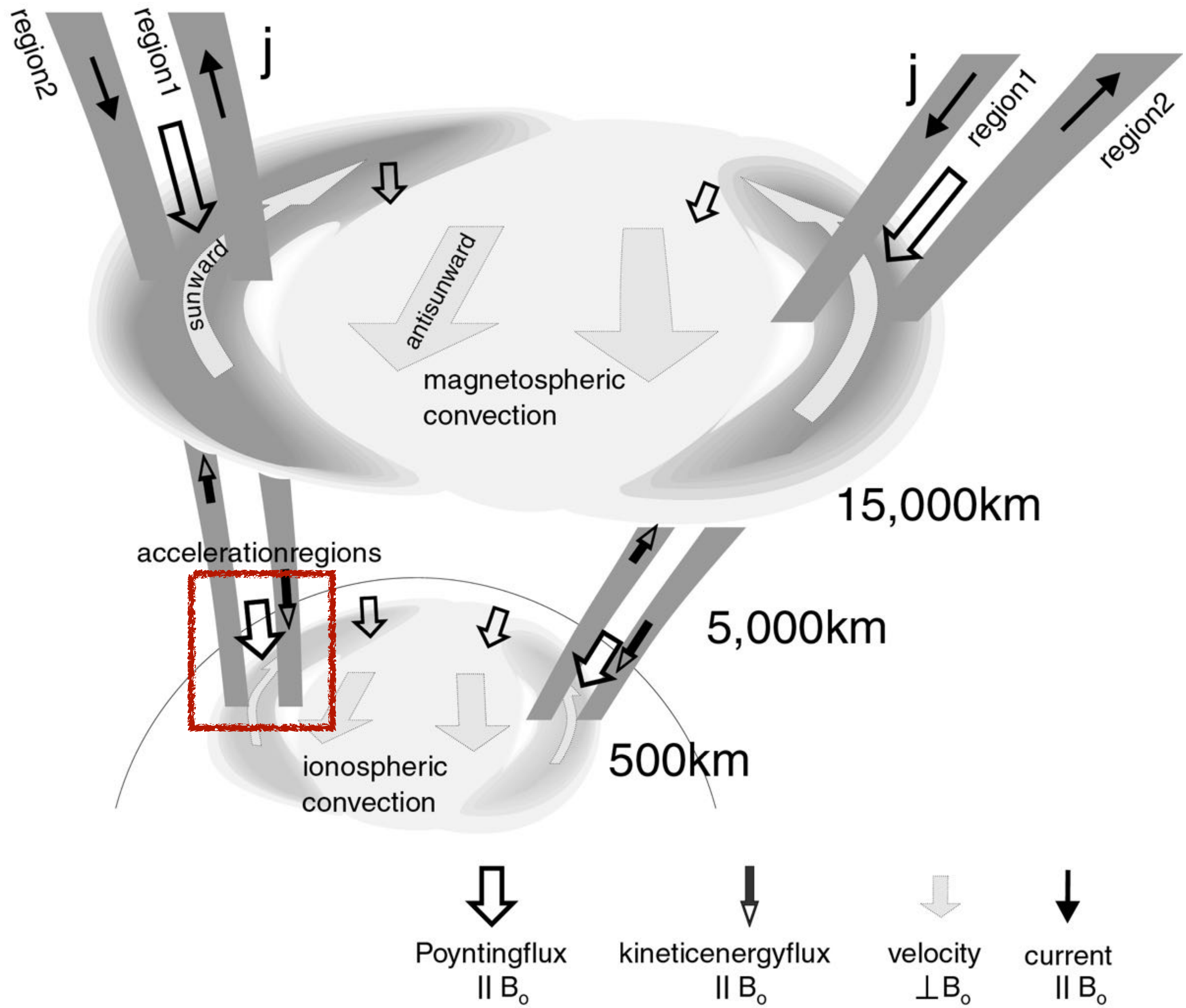

A. Vaivads, Ph.D. dissertation

Incoherent Scatter Radar (ISR)

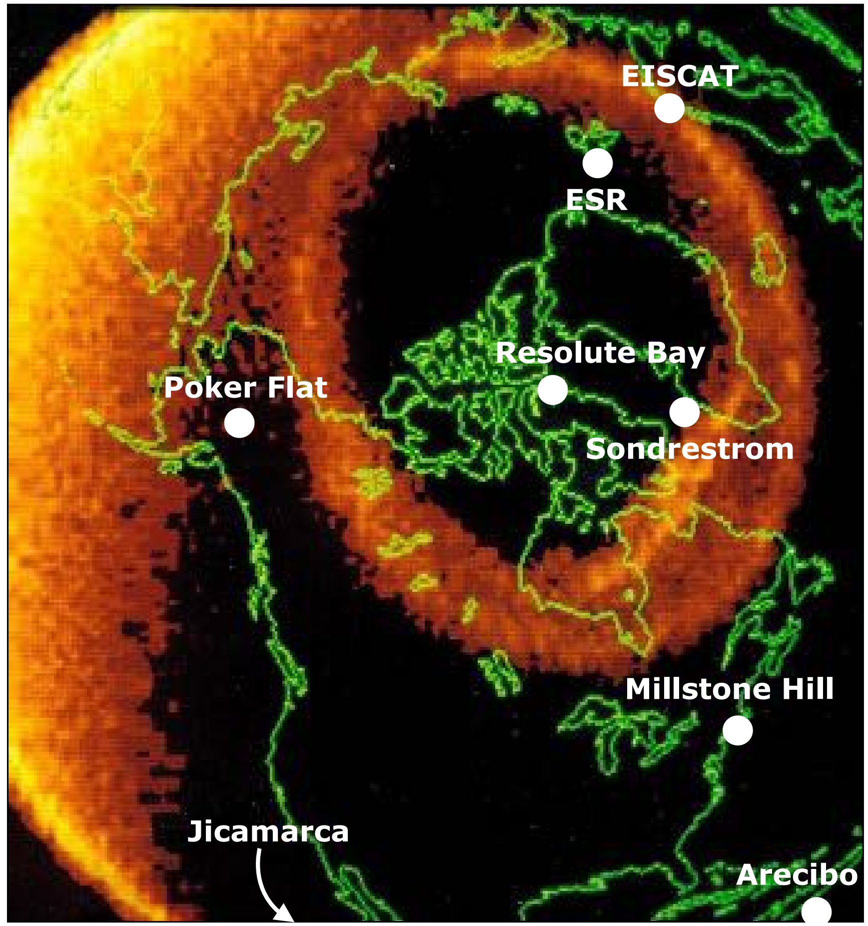

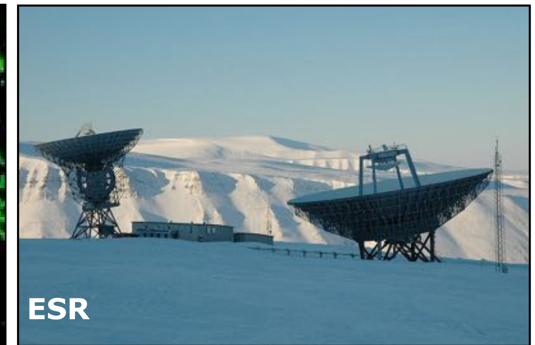

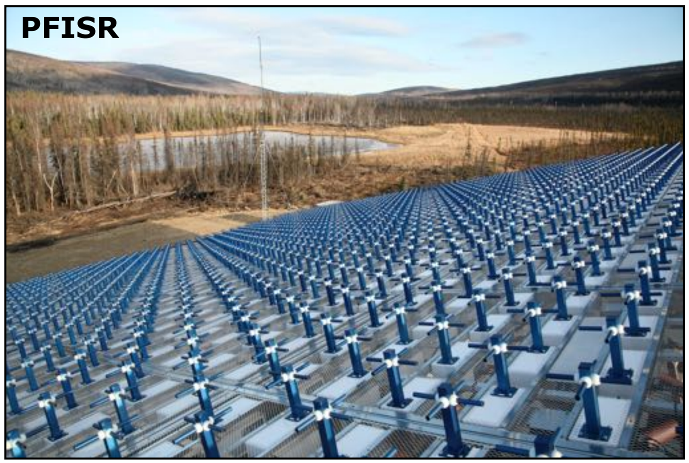

Optics!

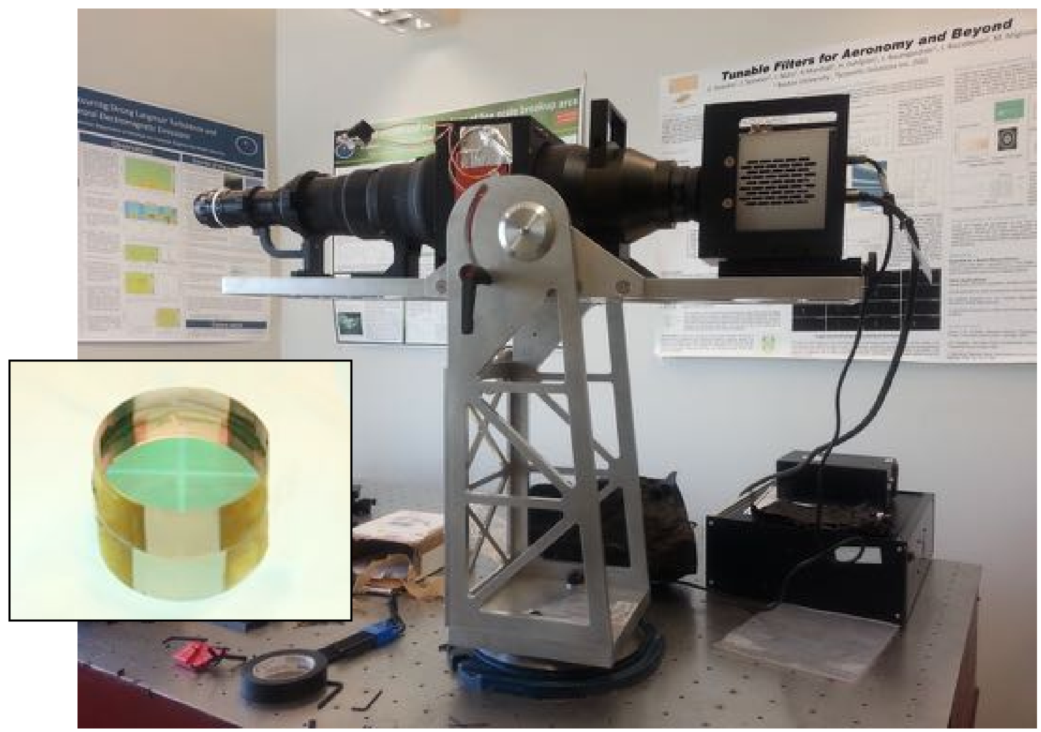

PFISR imaging beam patterns

26 beams

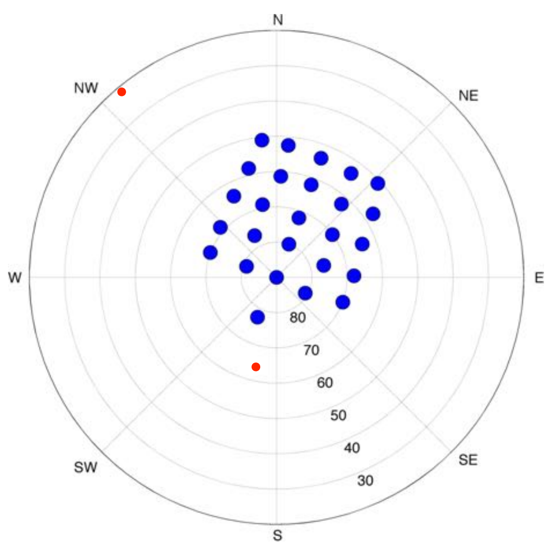

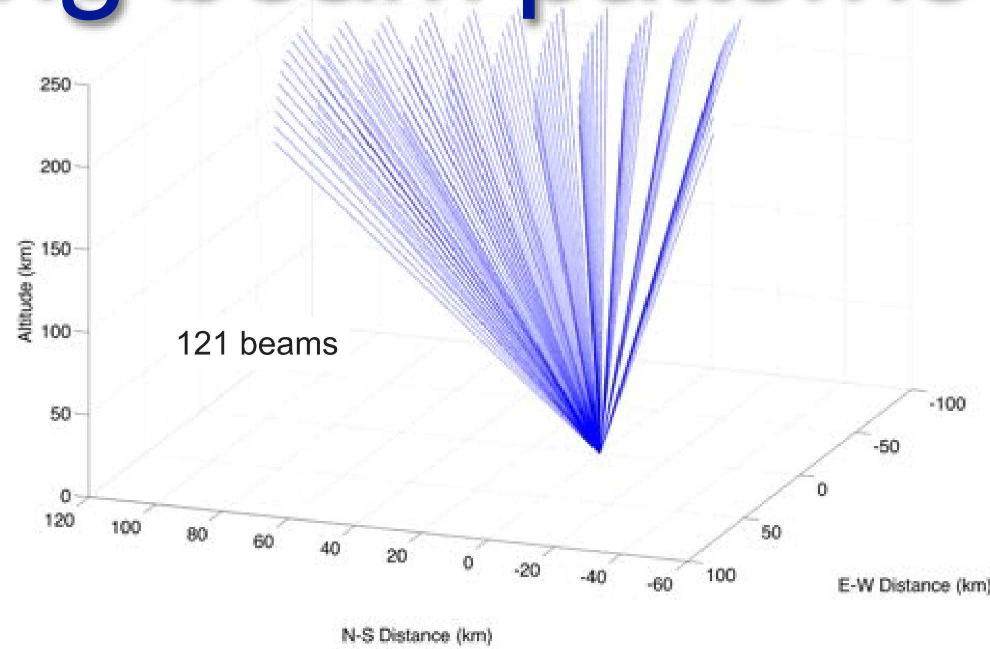

121 beams

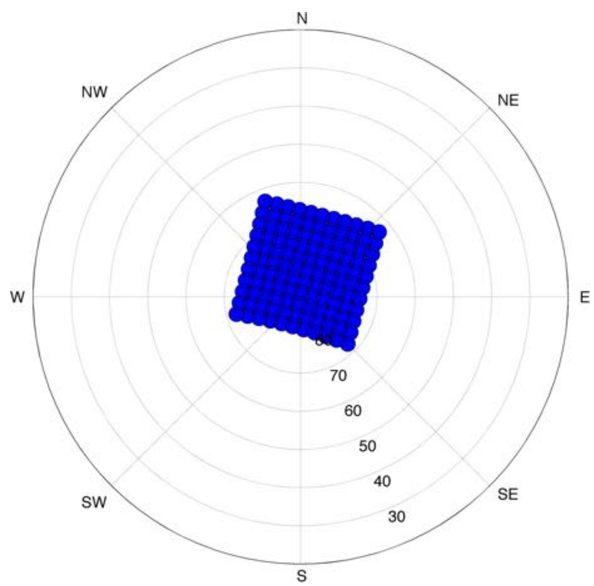

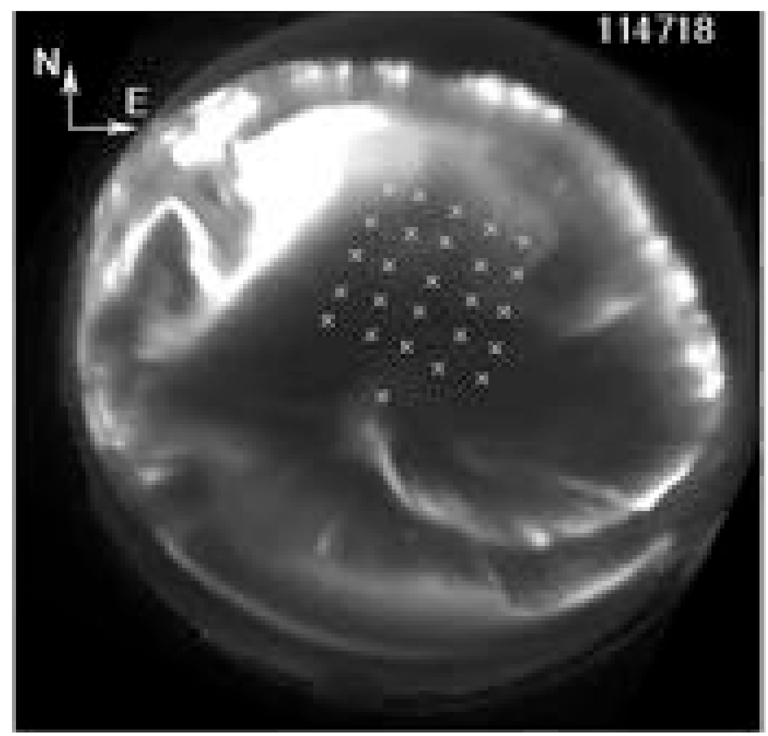

5-minute integration

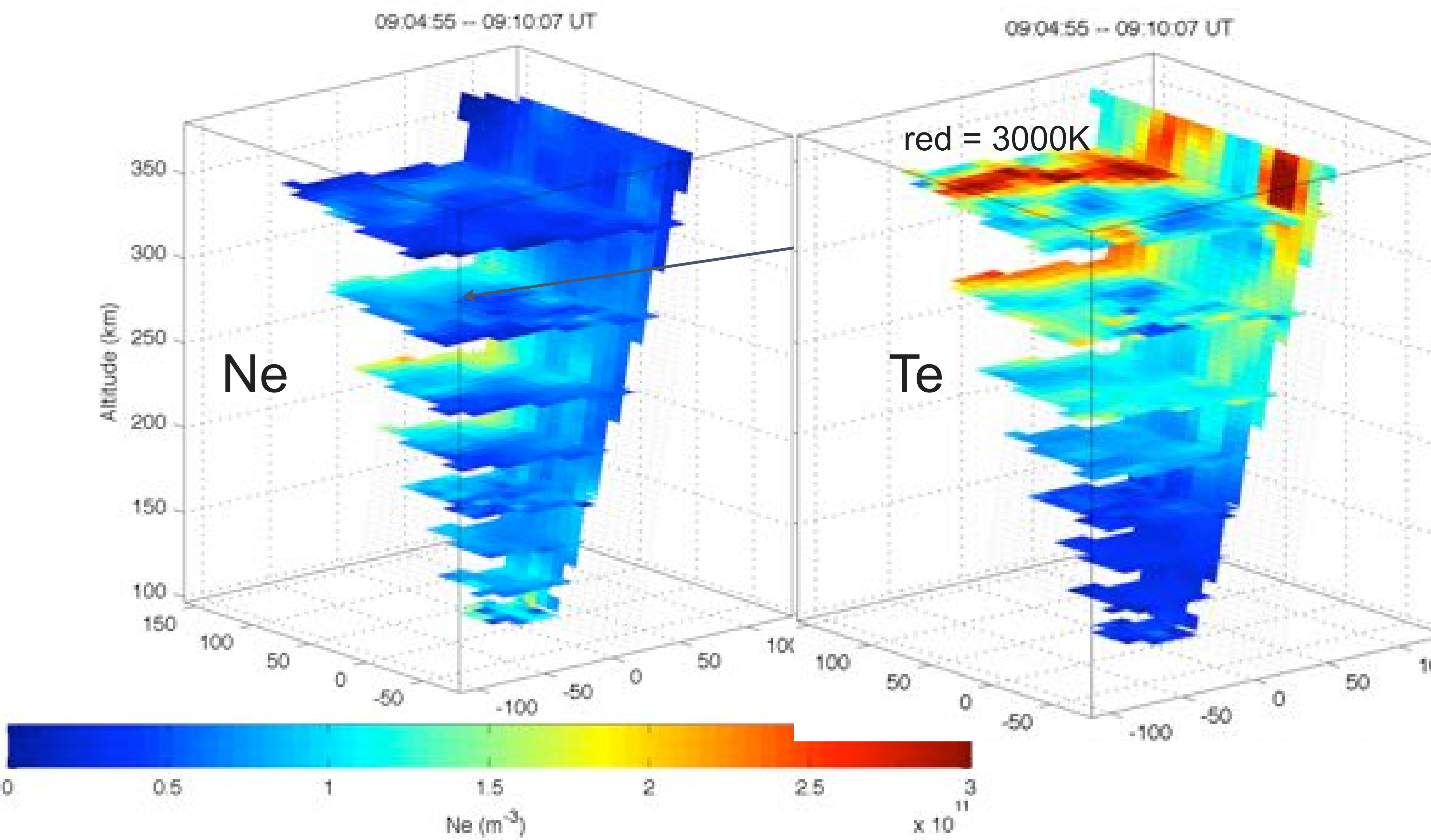

5-minute integration

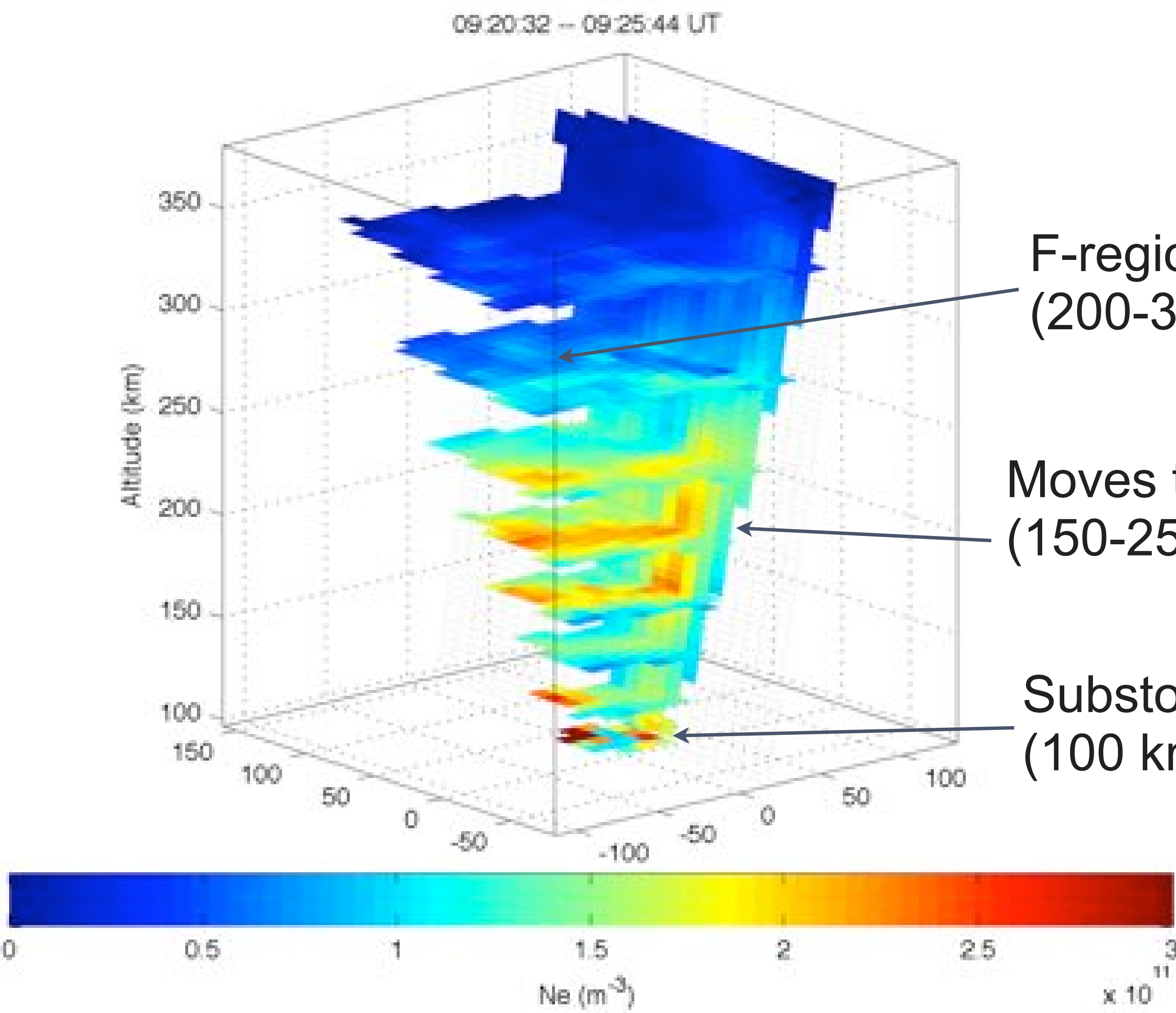

F-region production
(200-300 km, t-20min)

Moves to lower altitude
(150-250km, t-5min)

Substorm onset
(100 km)

5-minute integration

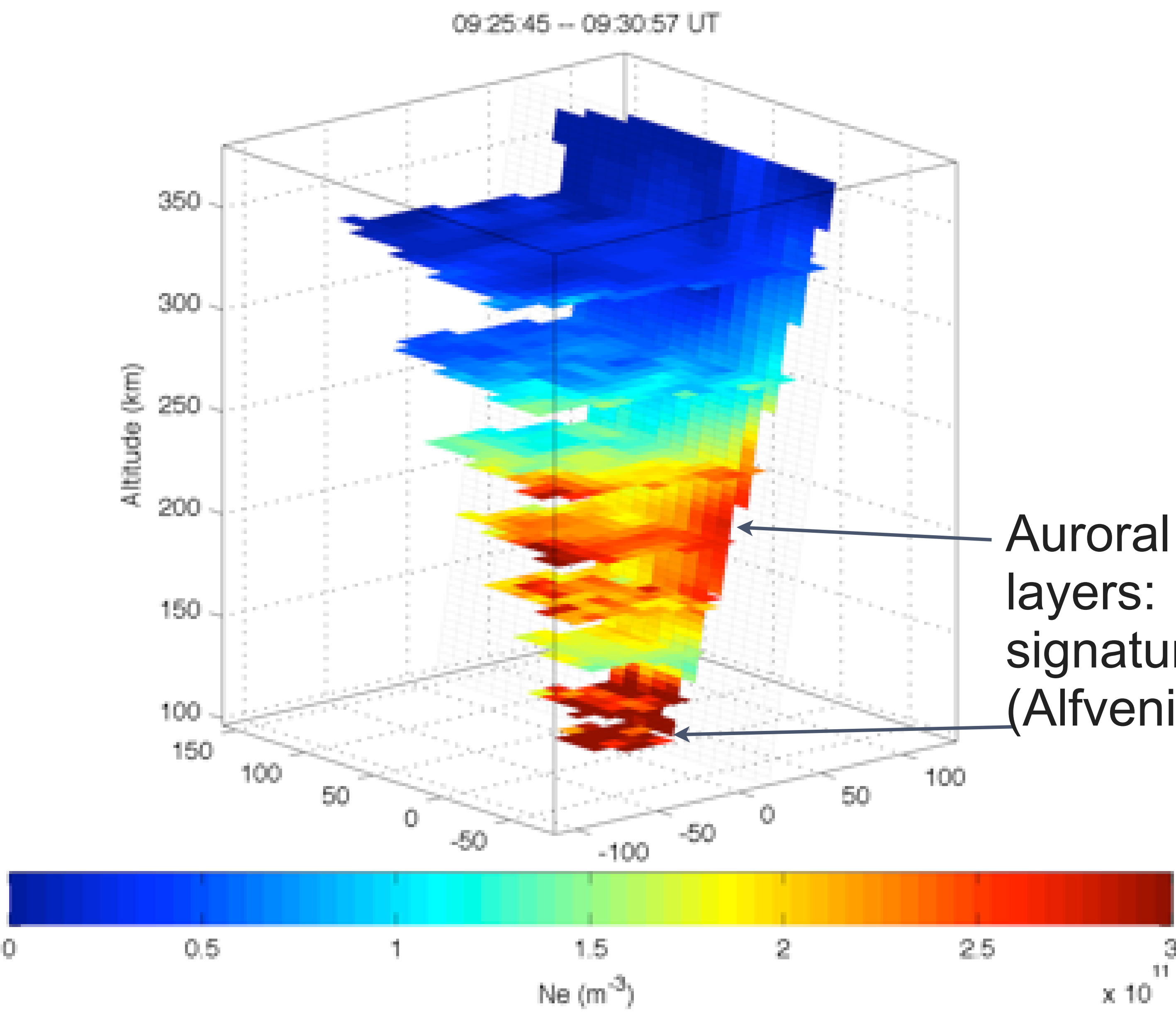

Auroral ionization in two layers:
signature of broad (Alfvenic) energy distribution

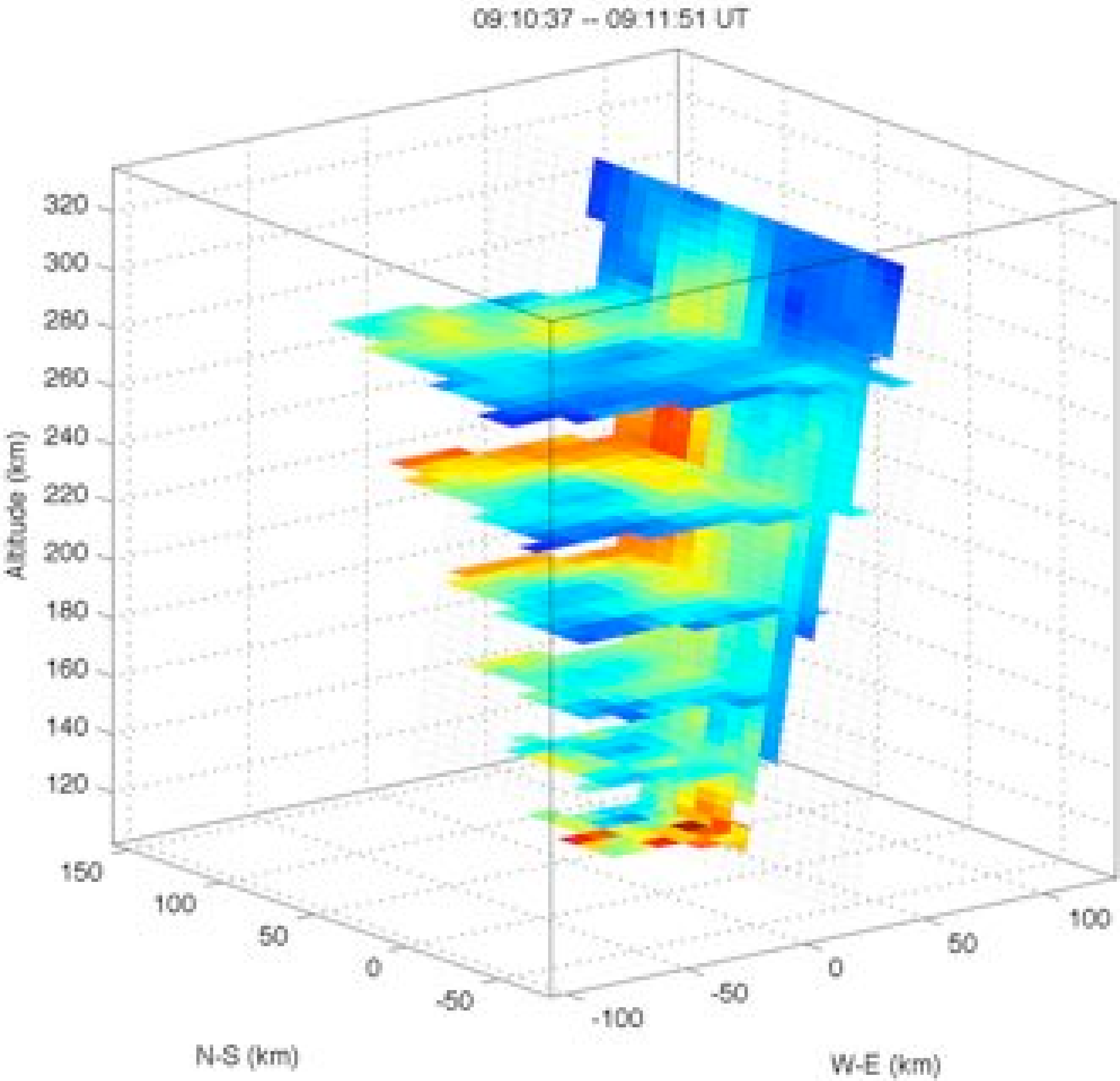
09:10:37 -- 09:11:51 UT
Altitude (km)
320
300
280
260
240
220
200
180
160
140
120
150
100
50
0
-50
N-S (km)
-100
-50
0
50
100
W-E (km)

09:10:37

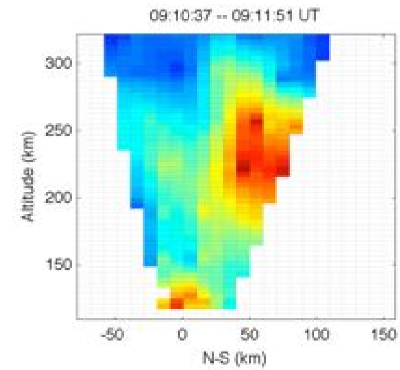
09:10:37 -- 09:11:51 UT
Altitude (km)
300
250
200
150
-50
0
50
100
150
N-S (km)

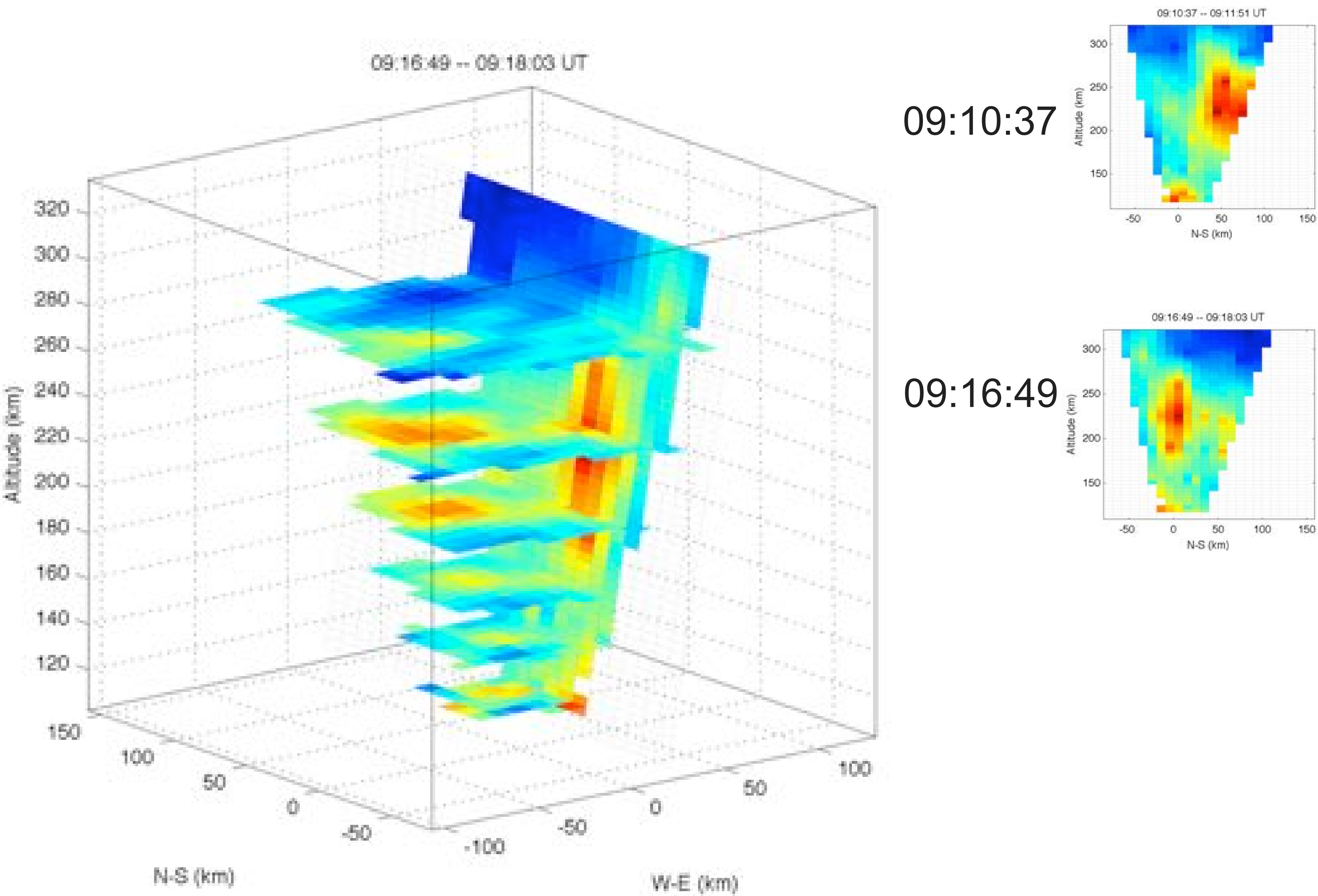
09:16:49 -- 09:18:03 UT
Altitude (km)
N-S (km)
W-E (km)
09:10:37
09:10:37 -- 09:11:51 UT
Altitude (km)
N-S (km)
09:16:49
09:16:49 -- 09:18:03 UT
Altitude (km)
N-S (km)

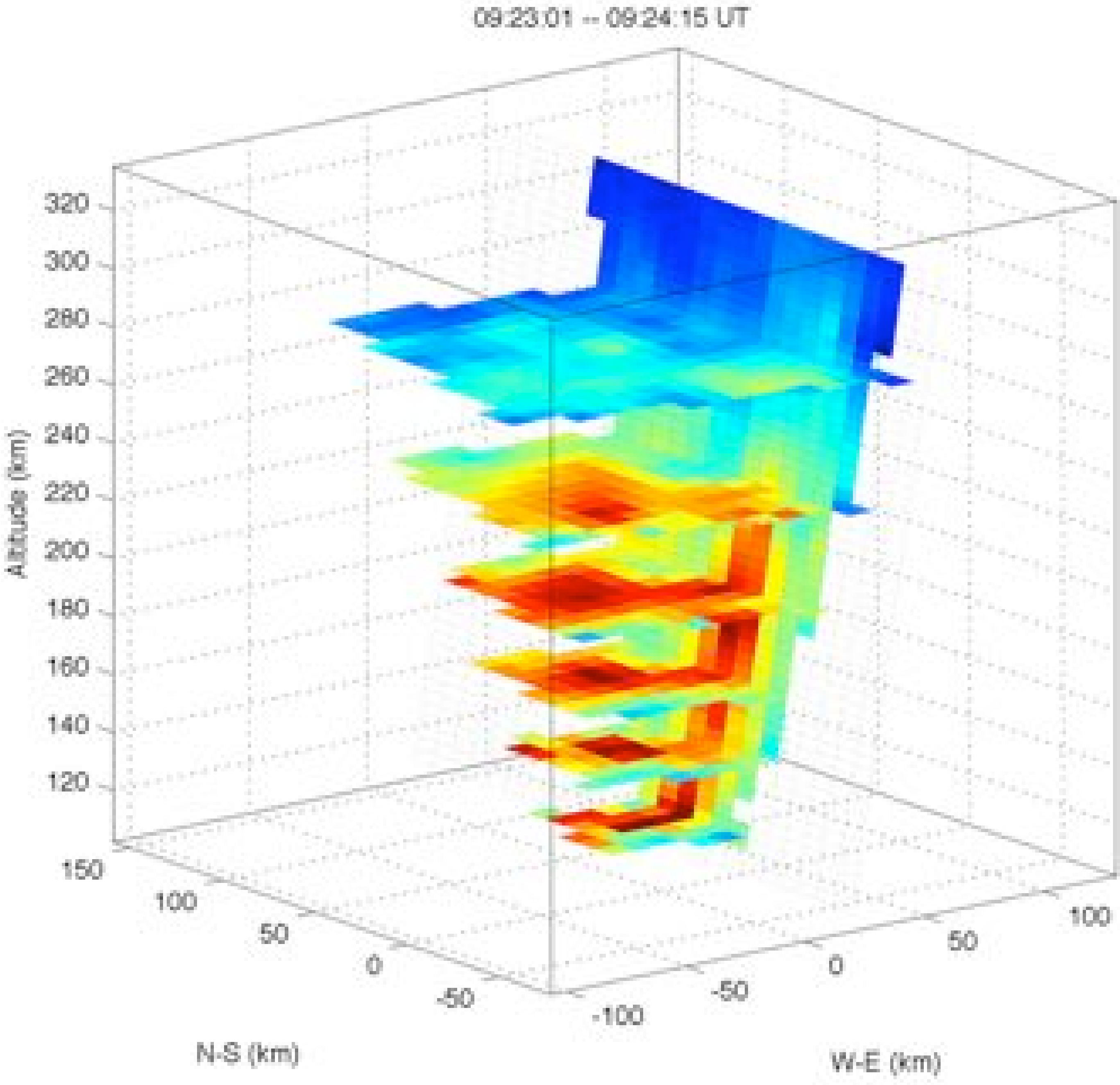

09:10:37

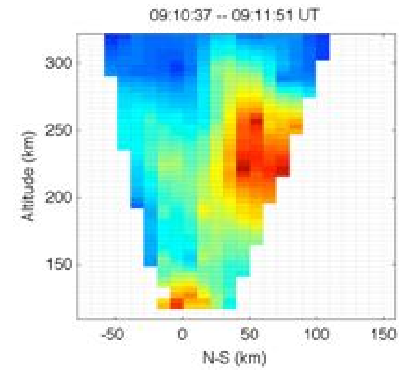

09:16:49

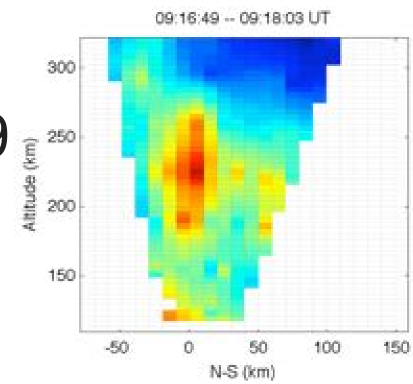

09:23:01

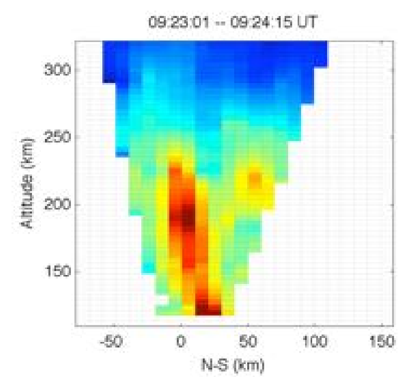

Semeter et al., JGR 2012, in review

Three-dimensional ionospheric imaging

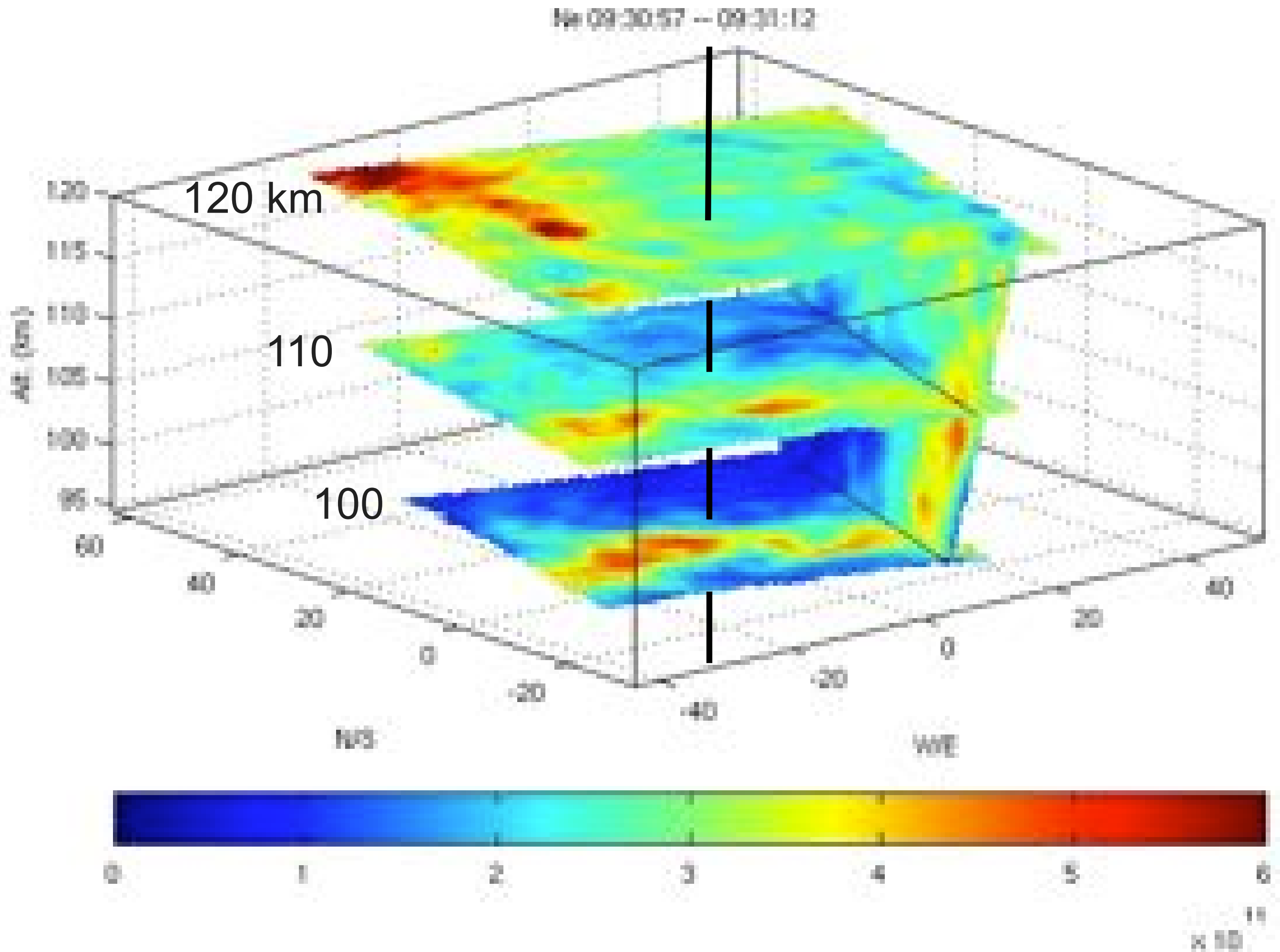

13-baud Barker Code
15-sec integration

Semeter et al., JASTP 2009

Ionospheric Flow Fields

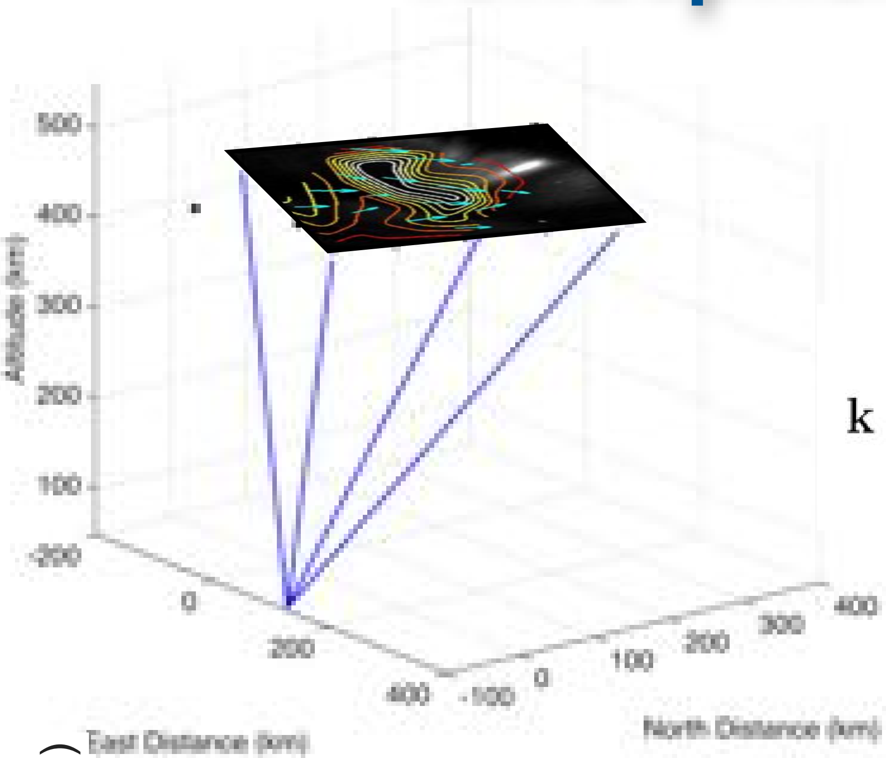

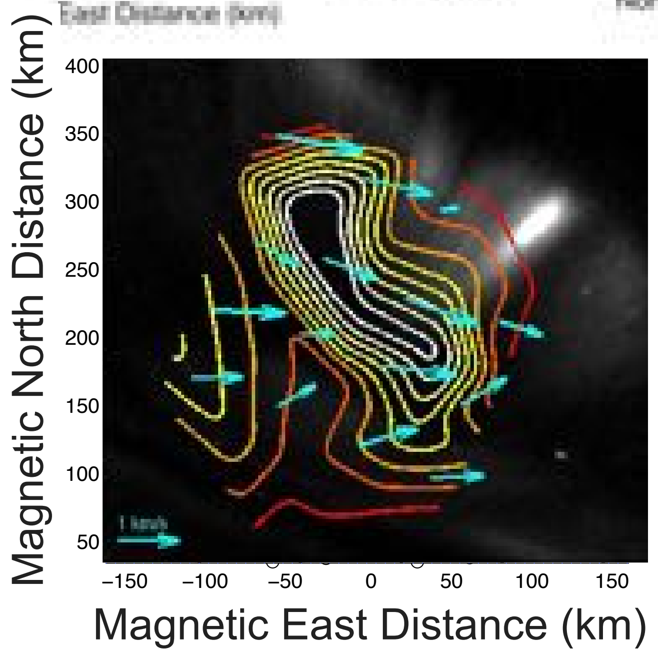

$$v_{los} = \mathbf{k} \cdot \begin{bmatrix} v_e & v_n & v_{\|} \end{bmatrix}^T$$

$$\mathbf{k} = \begin{bmatrix} \cos\theta\sin\phi \\ \cos\theta\cos\phi \\ \sin\theta \end{bmatrix}^T \begin{bmatrix} \cos\delta & \sin I \sin\delta & -\cos I \sin\delta \\ -\sin\delta & \cos\delta \sin I & -\cos I \cos\delta \\ 0 & \cos I & \sin I \end{bmatrix}$$

$$\begin{bmatrix} v_{los}^1 \\ v_{los}^2 \\ \vdots \\ v_{los}^i \\ \vdots \\ v_{los}^N \end{bmatrix} = \begin{bmatrix} \mathbf{k}^1 \\ \mathbf{k}^2 \\ \vdots \\ \mathbf{k}^i \\ \vdots \\ \mathbf{k}^N \end{bmatrix} \mathbf{v} + \begin{bmatrix} e_{los}^1 \\ e_{los}^2 \\ \vdots \\ e_{los}^i \\ \vdots \\ e_{los}^N, \end{bmatrix}$$

$$\mathbf{v}_{los} = A\mathbf{v} + \mathbf{e}_{los}$$

Semeter et al, JGRA 2010

Substorm poleward expansion

All-sky white light, 100x real time

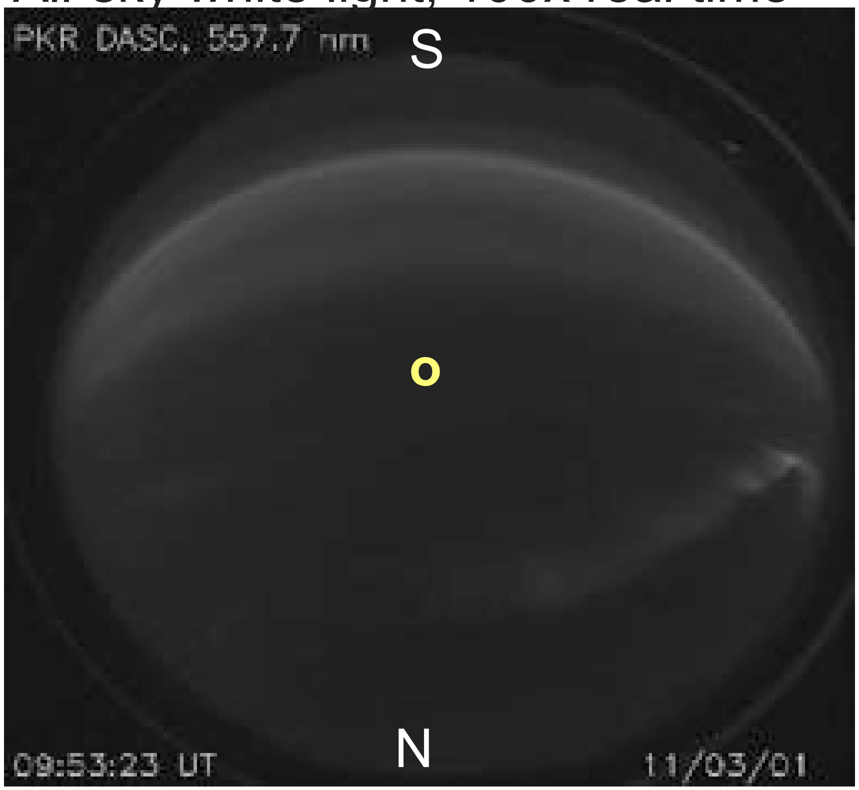

PFISR SNR (450MHz), 480us uncoded pulse

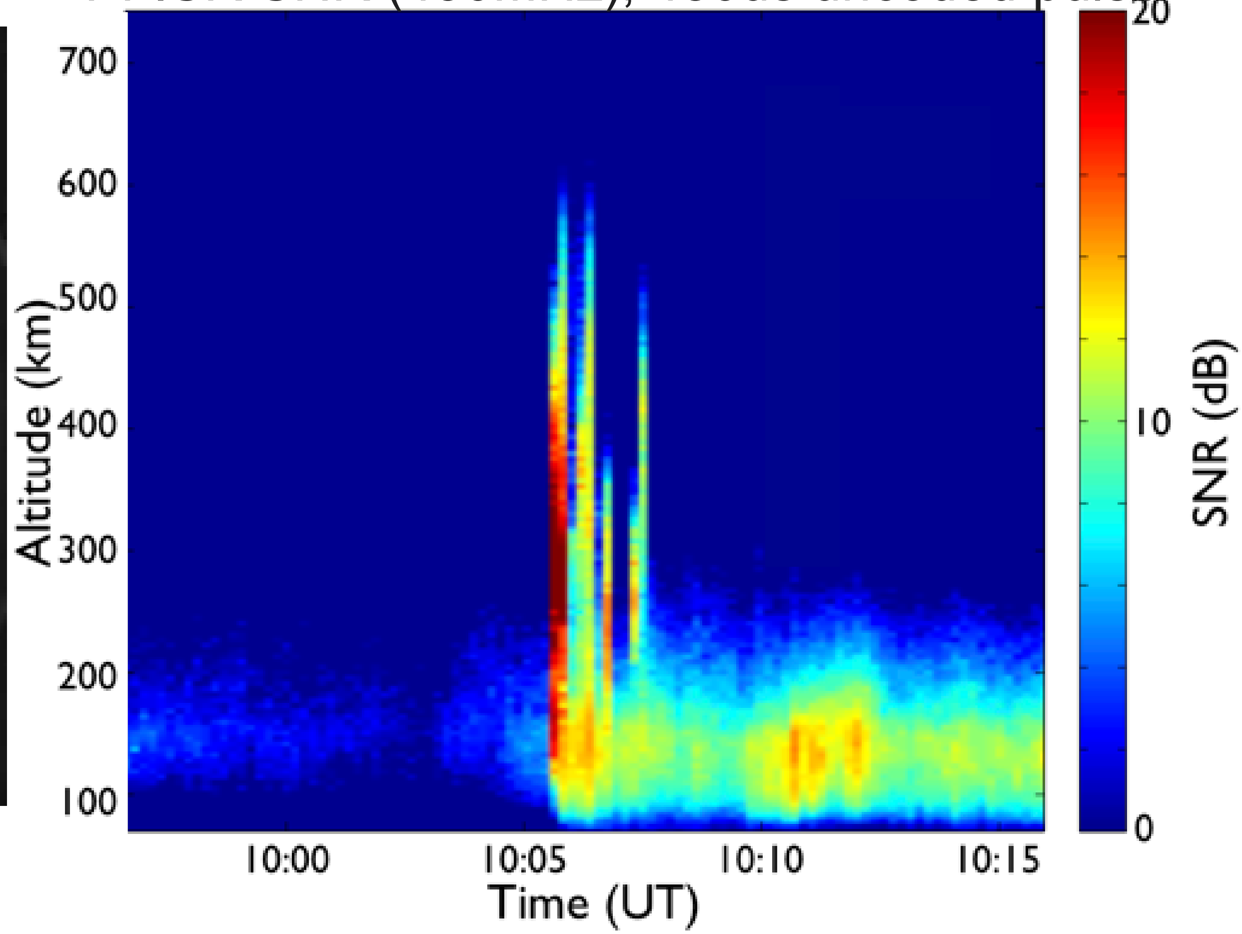

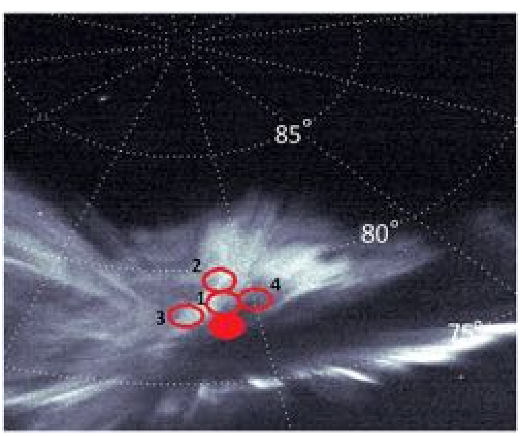

The auroras at the leading edge of the substorm expansion are correlated with coherent UHF backscatter, indicating destabilization of ion-acoustic waves by decay of Langmuir waves resonantly excited by low-energy electron fluxes.

Akbari et al., 2013

Radar perspective

All-sky 557.7nm, 100x real time

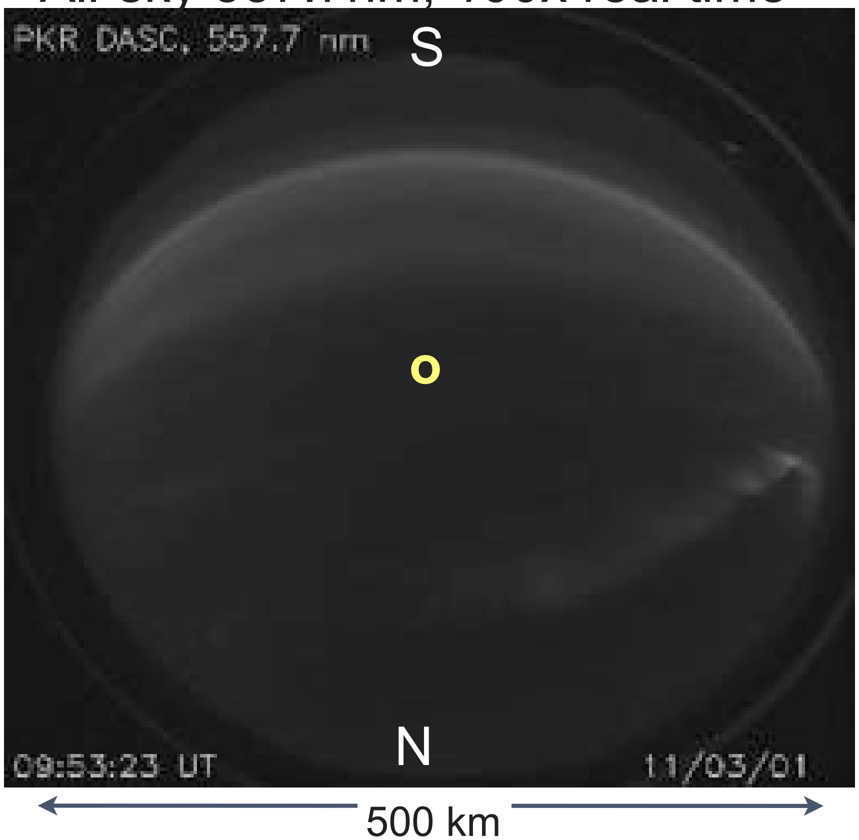

PFISR SNR (450MHz), 480us uncoded pulse

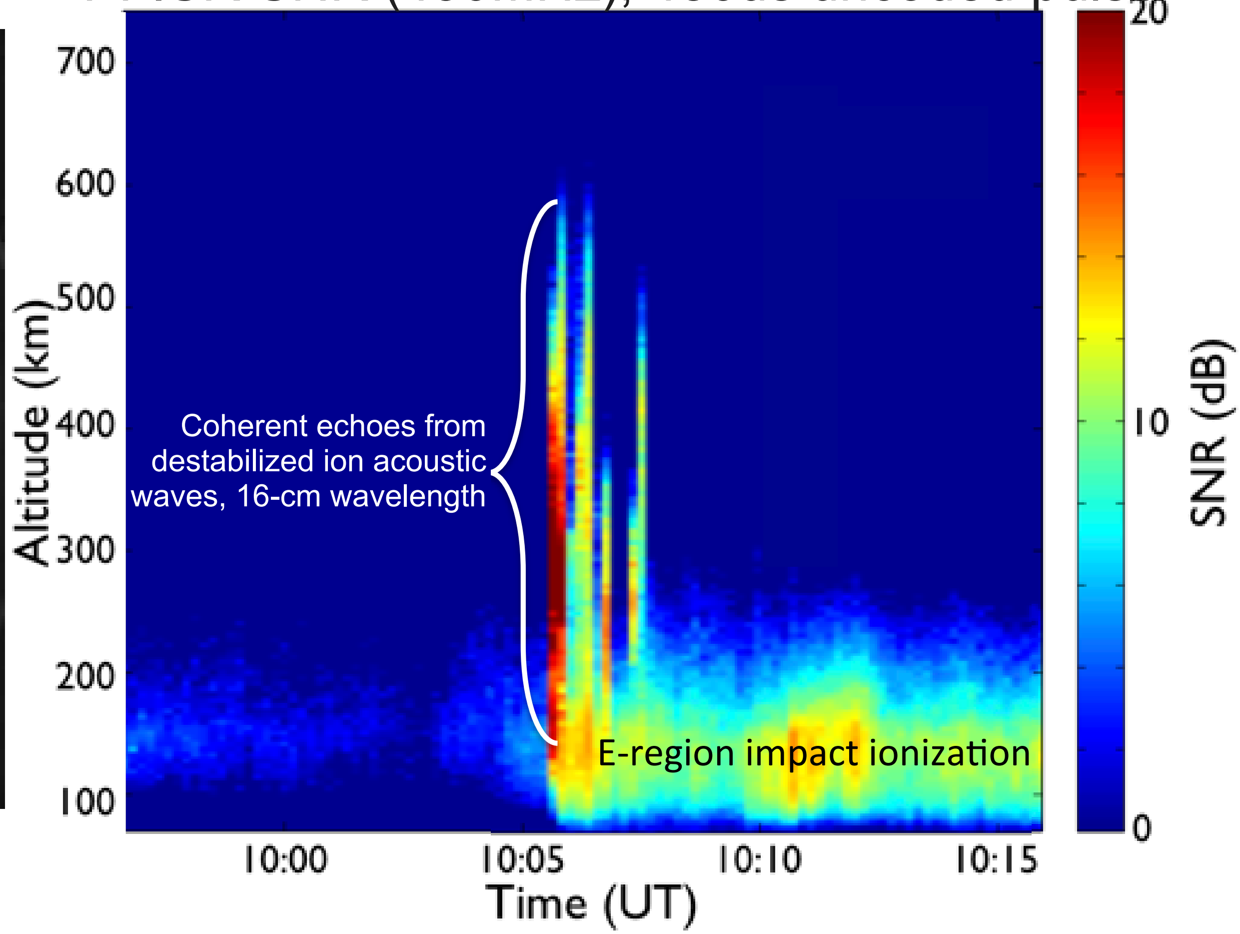

The auroras at the leading edge of the substorm expansion are correlated with coherent UHF backscatter, indicating destabilization of ion-acoustic waves by decay of Langmuir waves resonantly excited by low-energy electron fluxes.

Akbari et al., 2013

Radar perspective

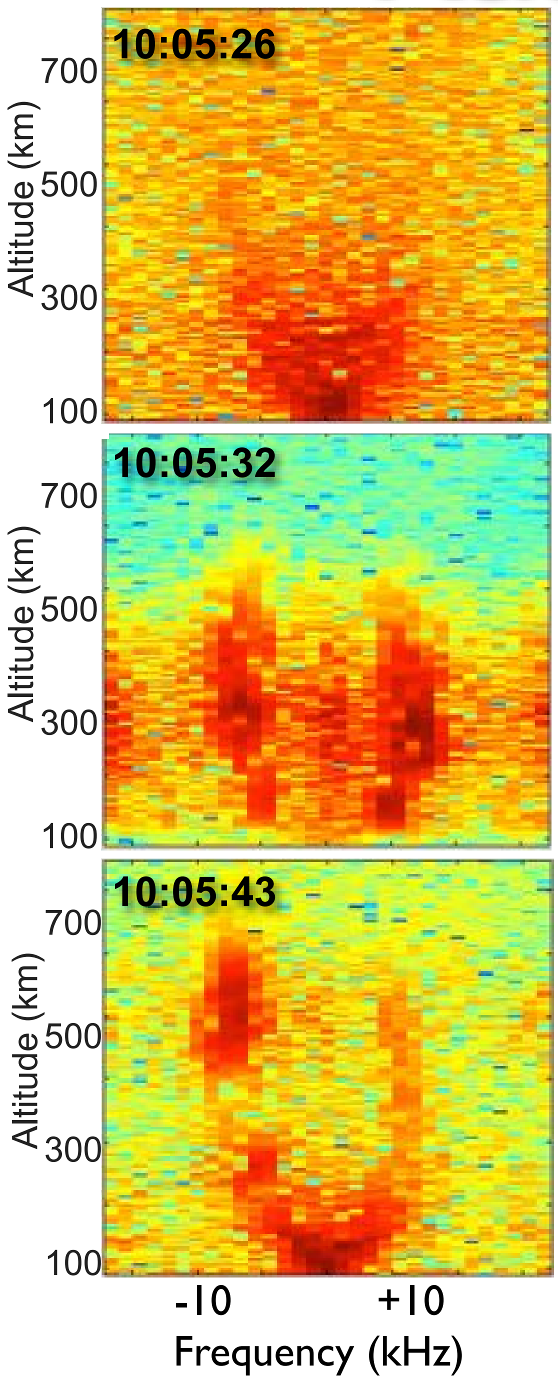

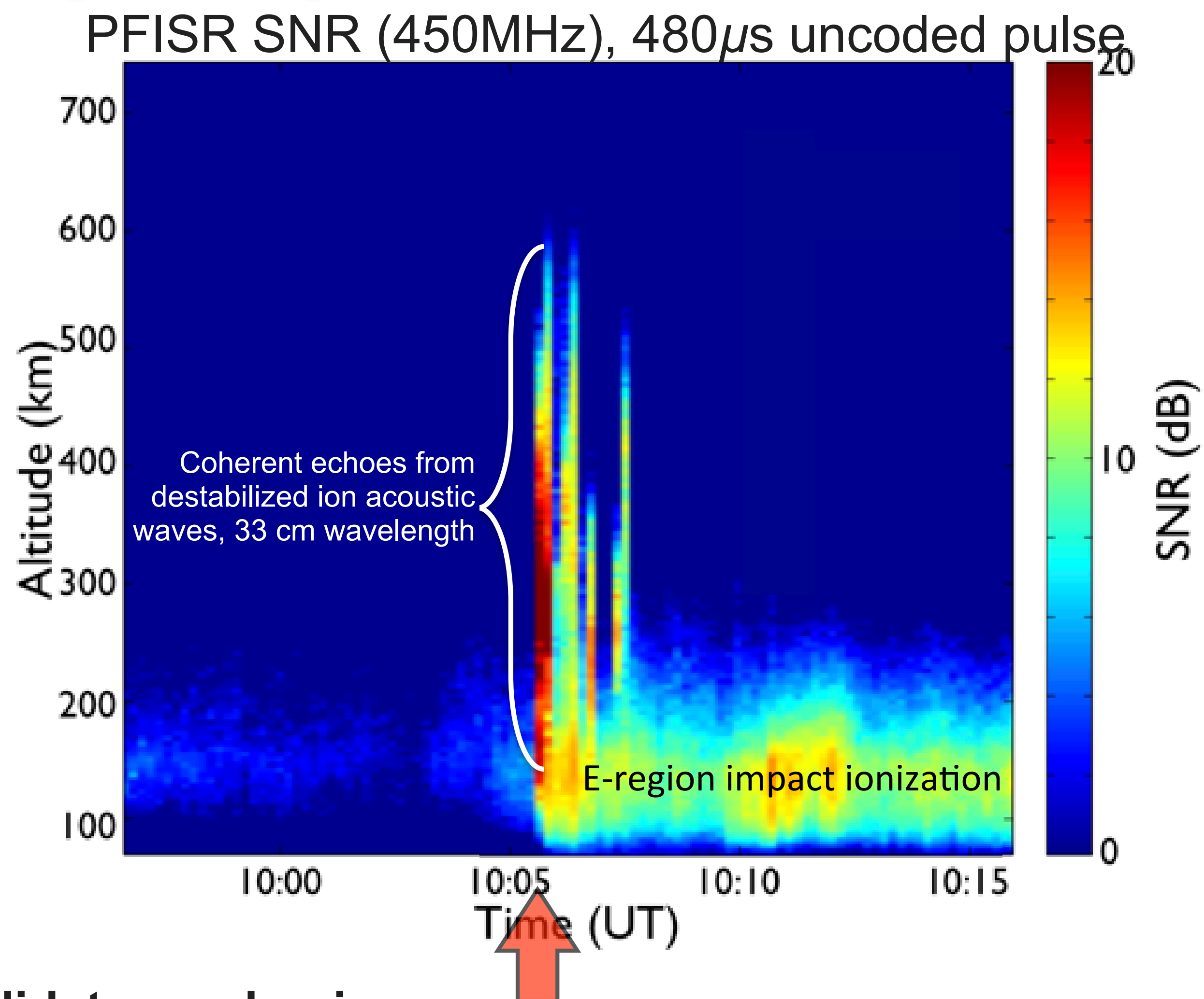

Candidate mechanisms:

1. Parametric decay of Langmuir turbulence (beam related)
2. ion-electron streaming instability (current related)

Akbari et al., 2013

Incoherent Scatter Radar (ISR)

Ion-acoustic

$$\omega_s = C_s k \qquad C_s = \sqrt{k_B(T_e + 3T_i)/m_i}$$

$$\omega_{si} = -\sqrt{\frac{\pi}{8}}\left[\left(\frac{m_e}{m_i}\right)^{\frac{1}{2}} + \left(\frac{T_e}{T_i}\right)^{\frac{3}{2}} \exp\left(-\frac{T_e}{2T_i} - \frac{3}{2}\right)\right]\omega_s$$

Langmuir

$$\omega_L = \sqrt{\omega_{pe}^2 + 3\,k^2\,v_{the}^2} \approx \omega_{pe} + \frac{3}{2} v_{the}\lambda_{De}k^2$$

$$\omega_{Li} \approx -\sqrt{\frac{\pi}{8}}\frac{\omega_{pe}^3}{k^3}\frac{1}{v_{the}^3} exp\left(-\frac{\omega_{pe}^2}{2k^2v_{the}^2} - \frac{3}{2}\right)\omega_L$$

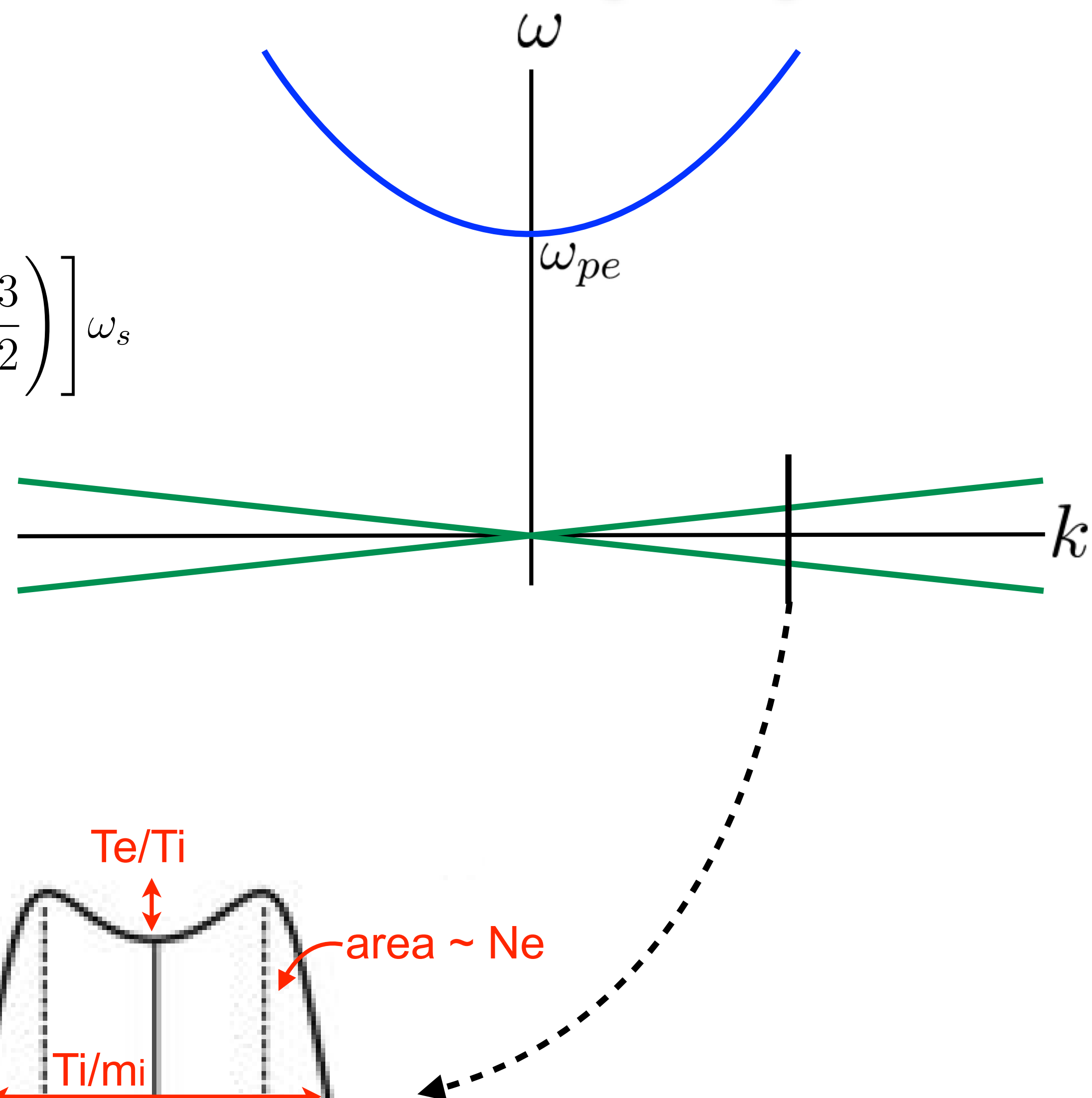

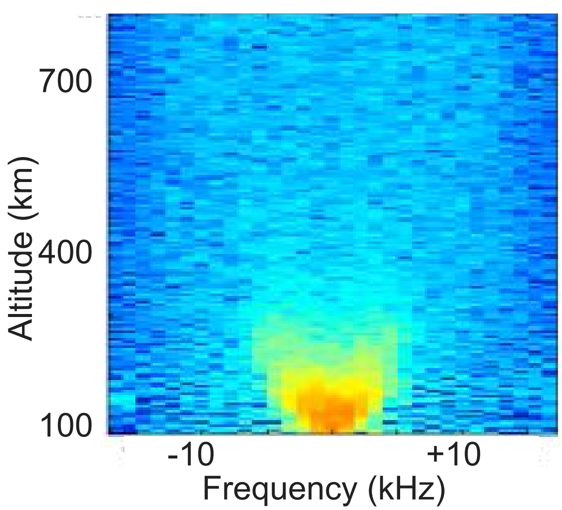

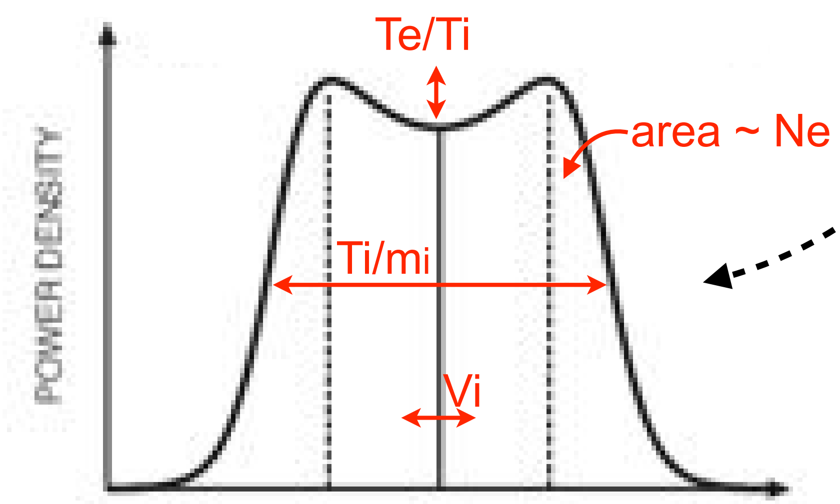

Non-thermal PFISR echoes

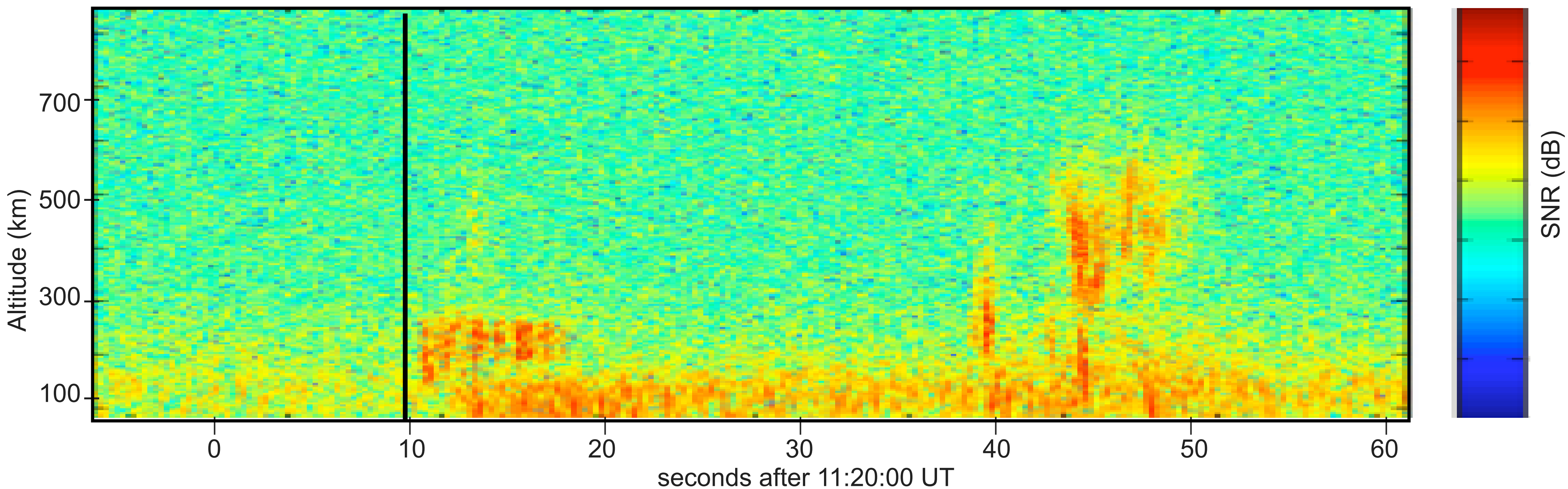

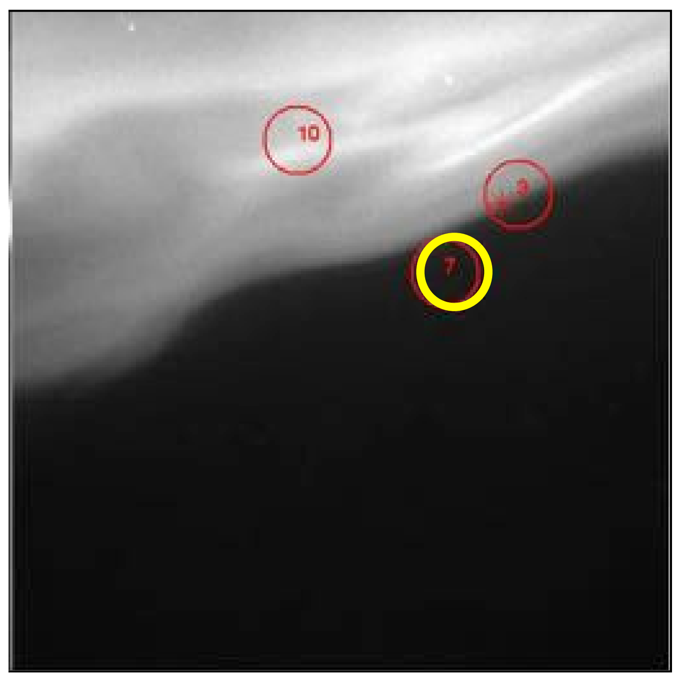

$11^o \times 11^o$
field-of view

21 x 21 km

Non-thermal PFISR echoes

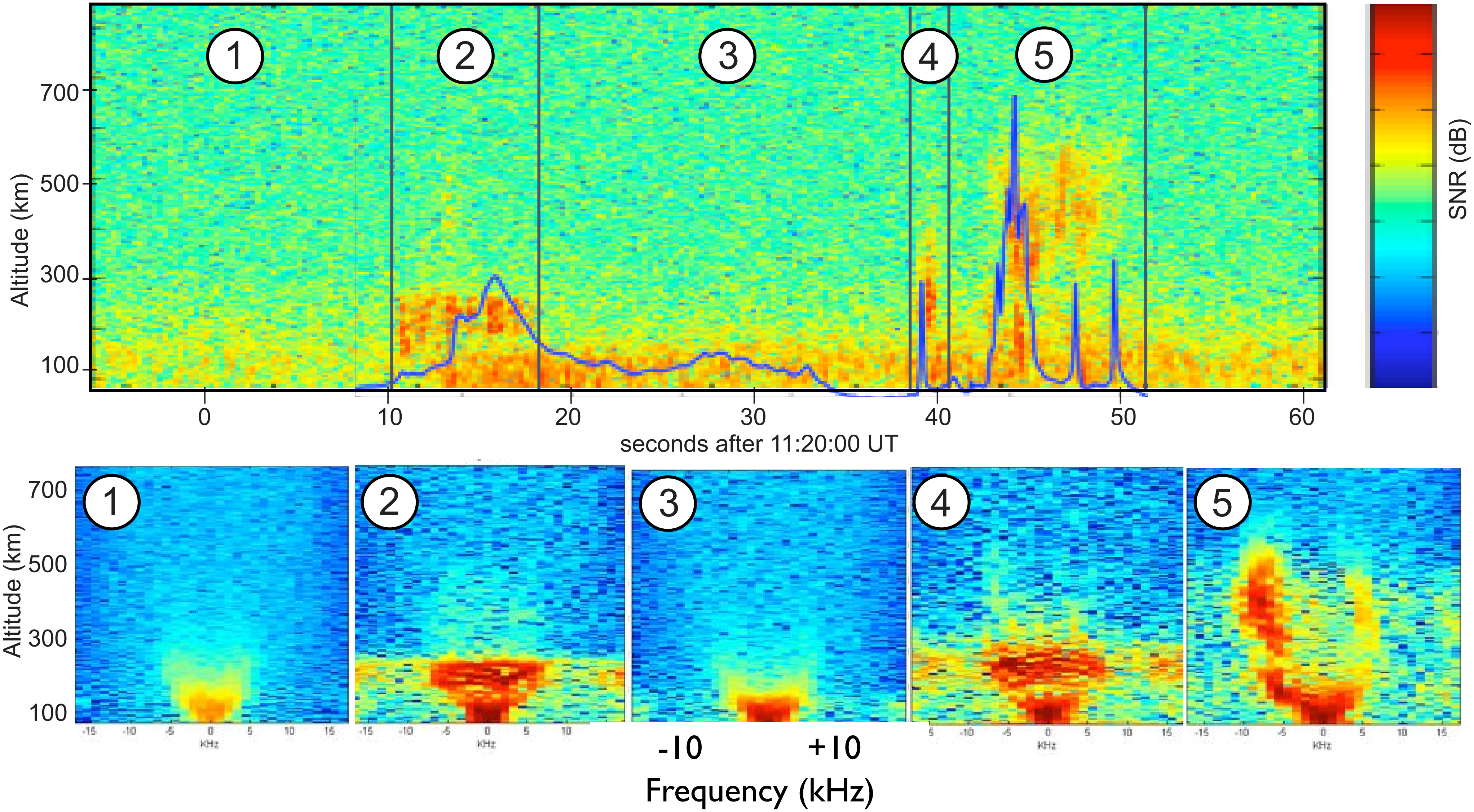

Akbari et al., GRL 2012

Ionospheric state parameters

All-sky white light, 100x real time

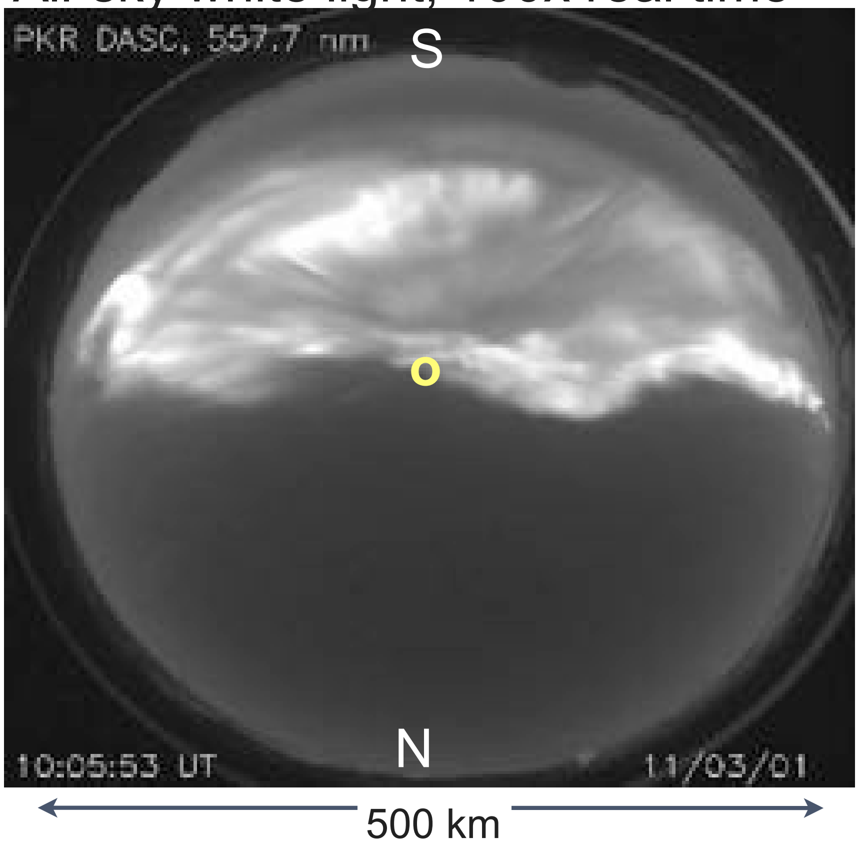

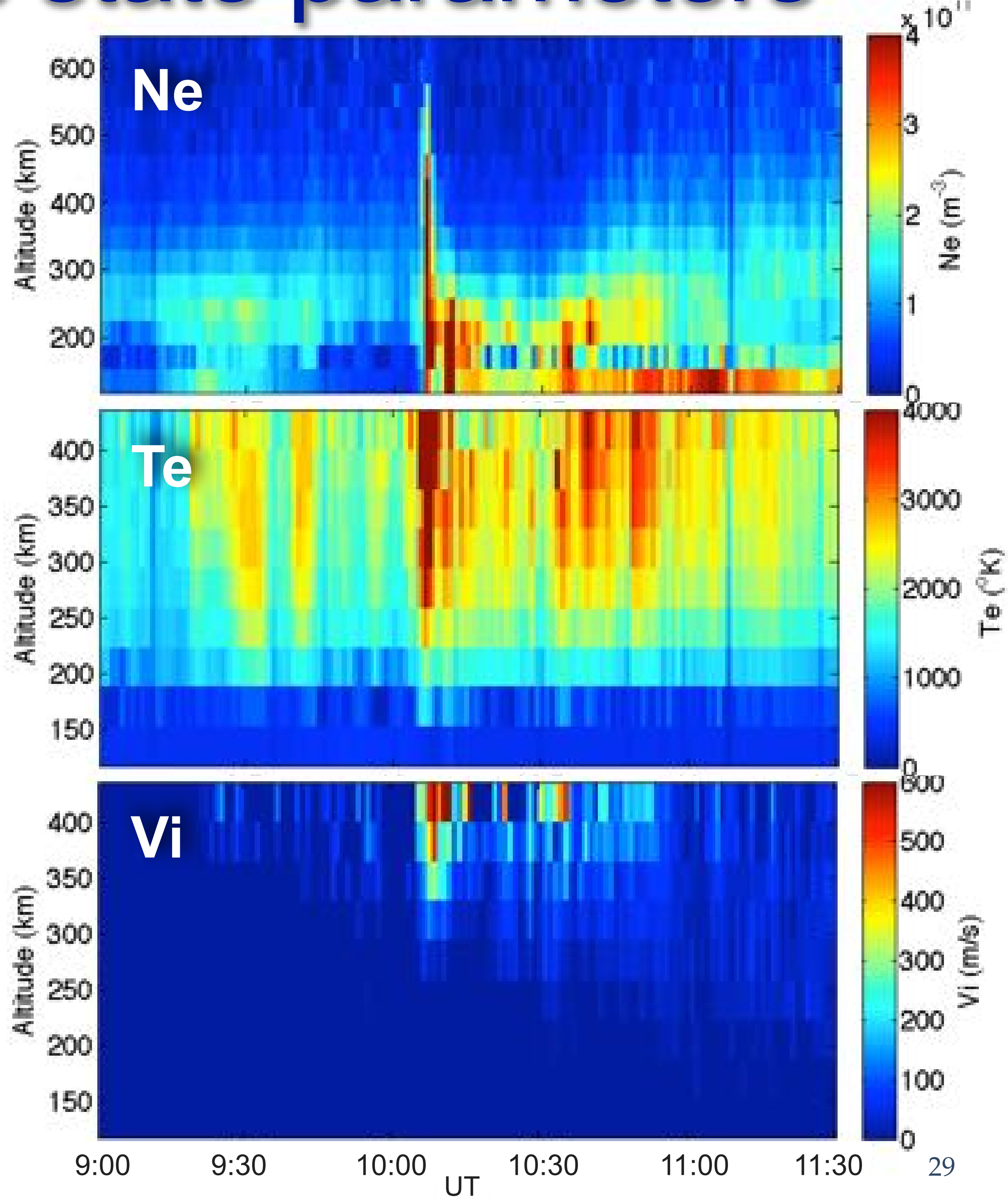

From Hawaii_2012_1.key

Cascading Langmuir Turbulence

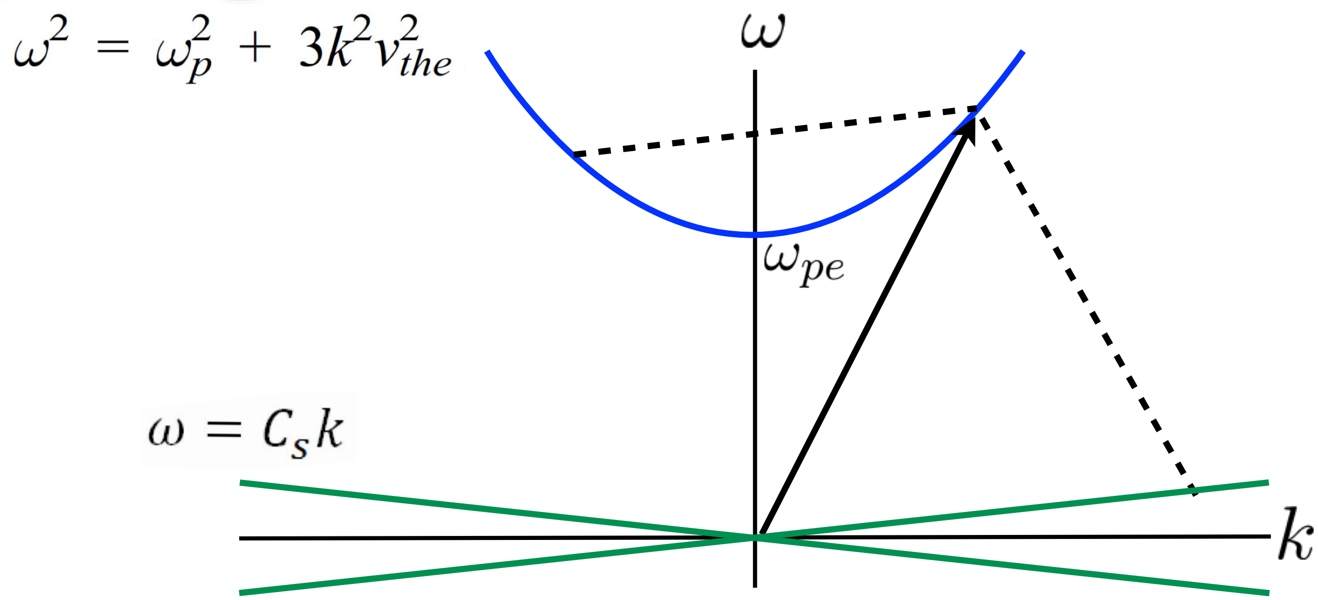

Parametric Decay Instability (PDI): an initial (mother) LW decay into another LW (daughter) and an ion-acoustic wave

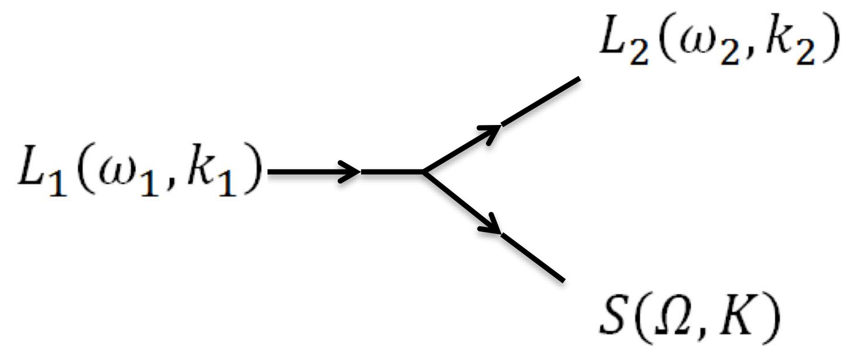

In this 3-wave interaction, energy and momentum are conserved

$$\begin{pmatrix}\omega_1 \\ k_1\end{pmatrix} = \begin{pmatrix}\omega_2 \\ k_2\end{pmatrix} + \begin{pmatrix}\Omega \\ K\end{pmatrix}$$

Cascading Langmuir Turbulence

$$\omega^2 = \omega_p^2 + 3k^2 v_{the}^2$$

Once the daughter LW increases in intensity to the PDI threshold, It also decays into another Ion Acoustic was and another LW.

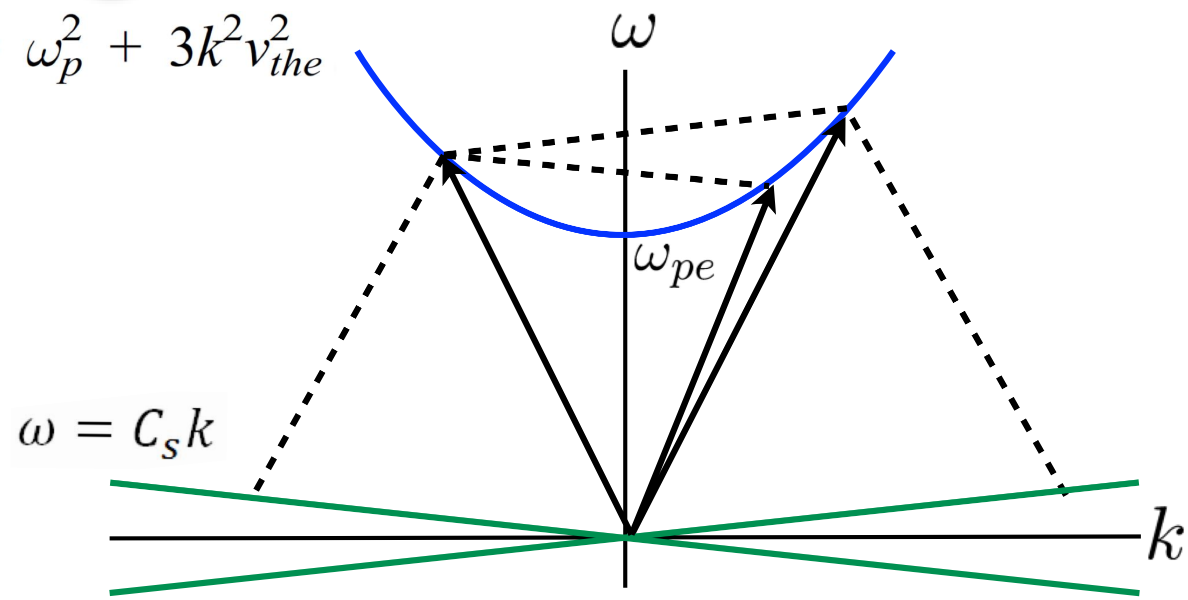

Parametric Decay Instability (PDI): an initial (mother) LW decay into another LW (daughter) and an ion-acoustic wave

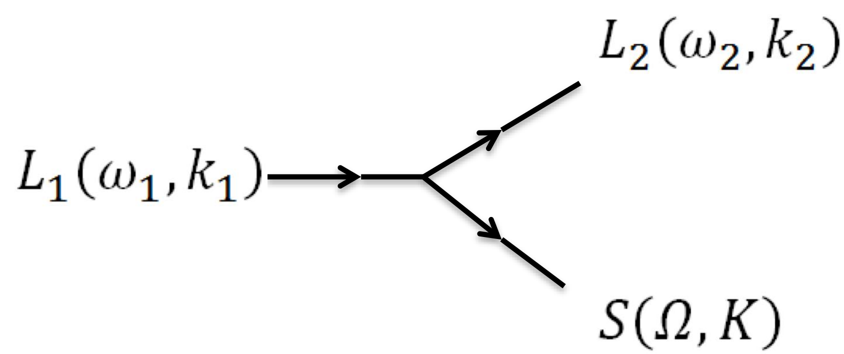

In this 3-wave interaction, energy and momentum are conserved

$$\begin{pmatrix}\omega_1\\k_1\end{pmatrix} = \begin{pmatrix}\omega_2\\k_2\end{pmatrix} + \begin{pmatrix}\Omega\\K\end{pmatrix}$$

Cascading Langmuir Turbulence

$$\omega^2 = \omega_p^2 + 3k^2 v_{the}^2$$

Provided there is enough energy pumped into the system, this process continues and the energy cascades toward smaller wave number (larger wavelength) until it reaches k=0, where the PDI is replaced by other instabilities.

$$\omega = C_s k$$

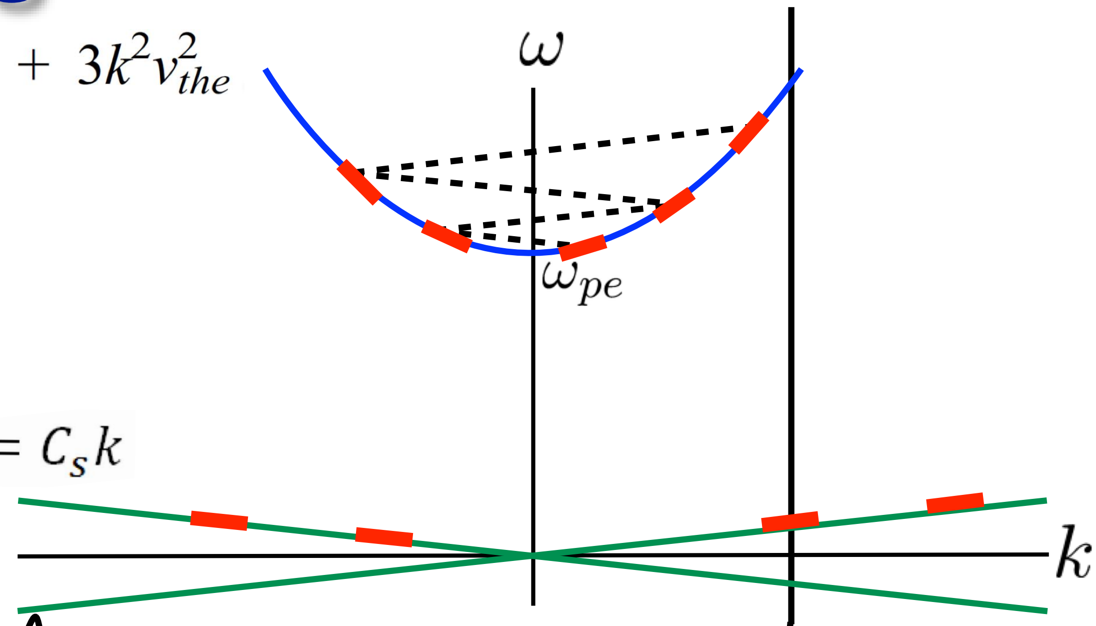

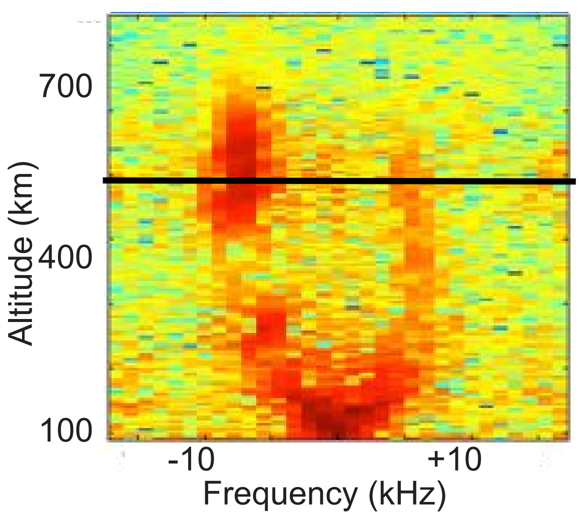

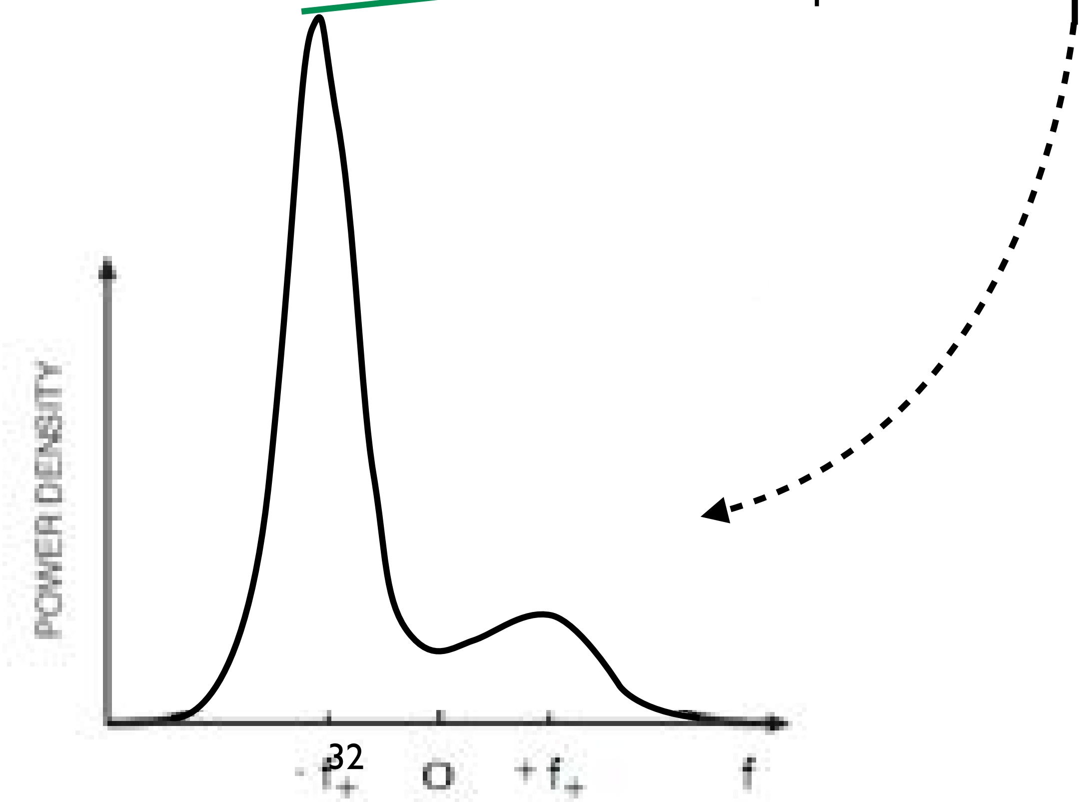

Cavitating Langmuir Turbulence

The non-linear phase of the modulational instability leads to formation of cavities/cavitons

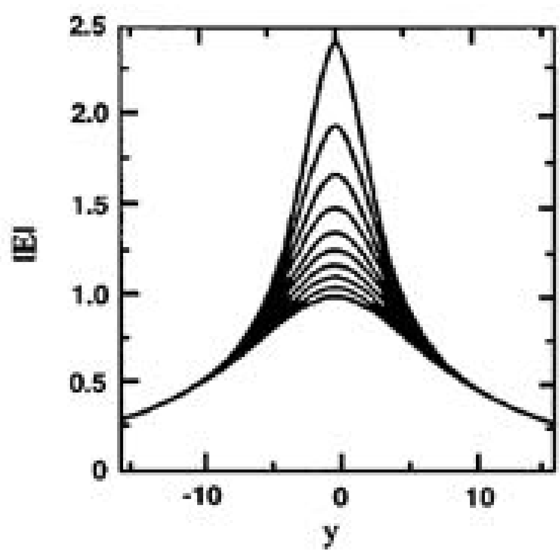

3D simulation

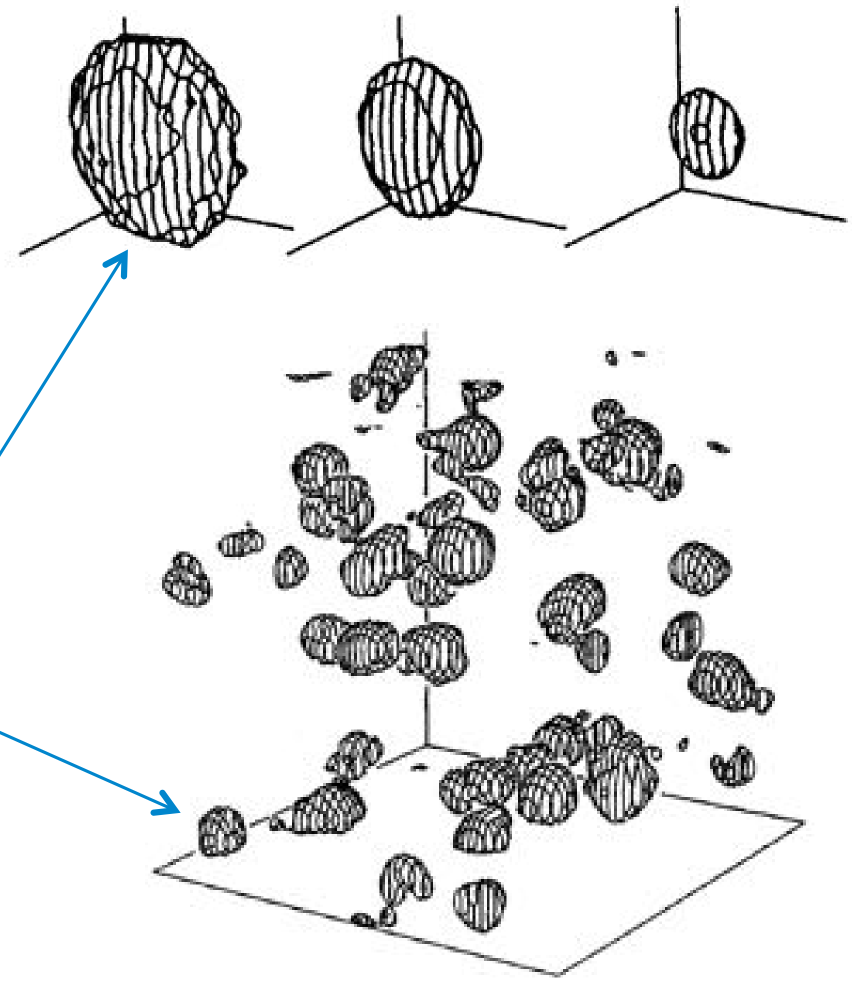

Surfaces of constant energy
Density (10% of the Max.)

[Robinson, 2006]

Cavitating Langmuir Turbulence

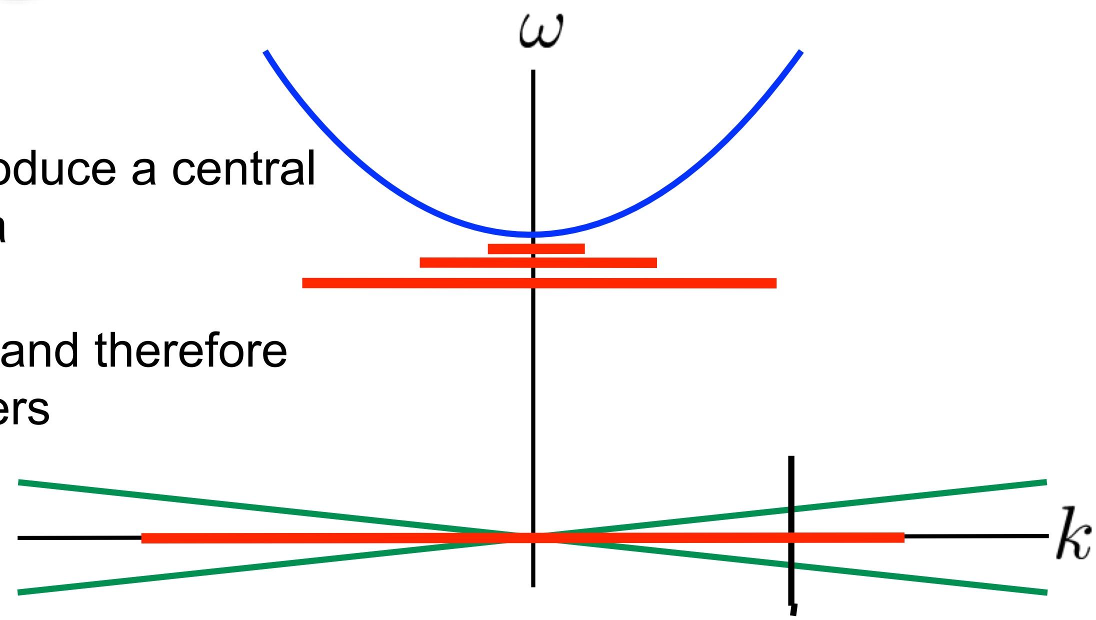

Cavities are stationary, therefore they only produce a central peak with zero Doppler in ISR ion-line spectra

Cavities become deeper and smaller in scale and therefore they transfer the energy to higher wavenumbers

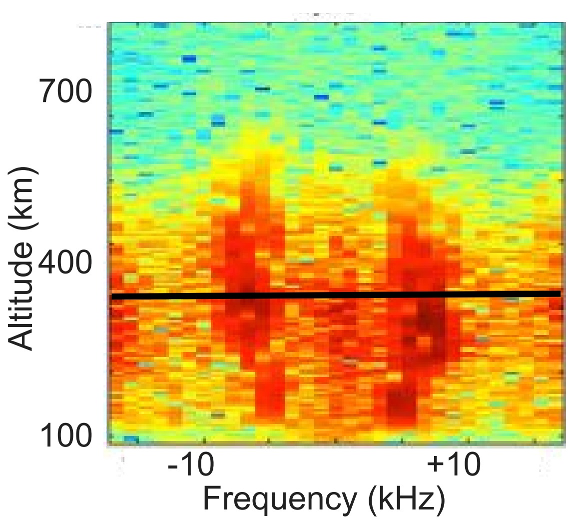

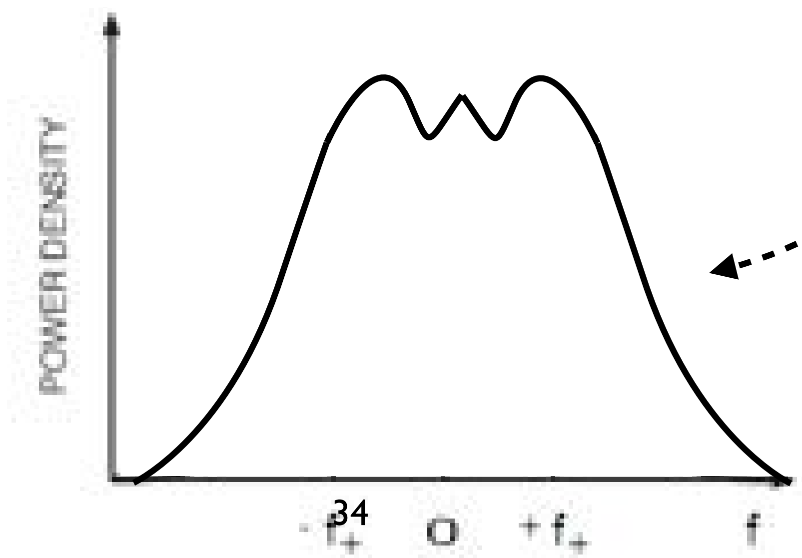

Energy dissipation is a multi-scale process

There is not a continuum of scales in the magnetosphere-ionosphere system. Rather, the physics changes abruptly as we cross specific parameter regimes.

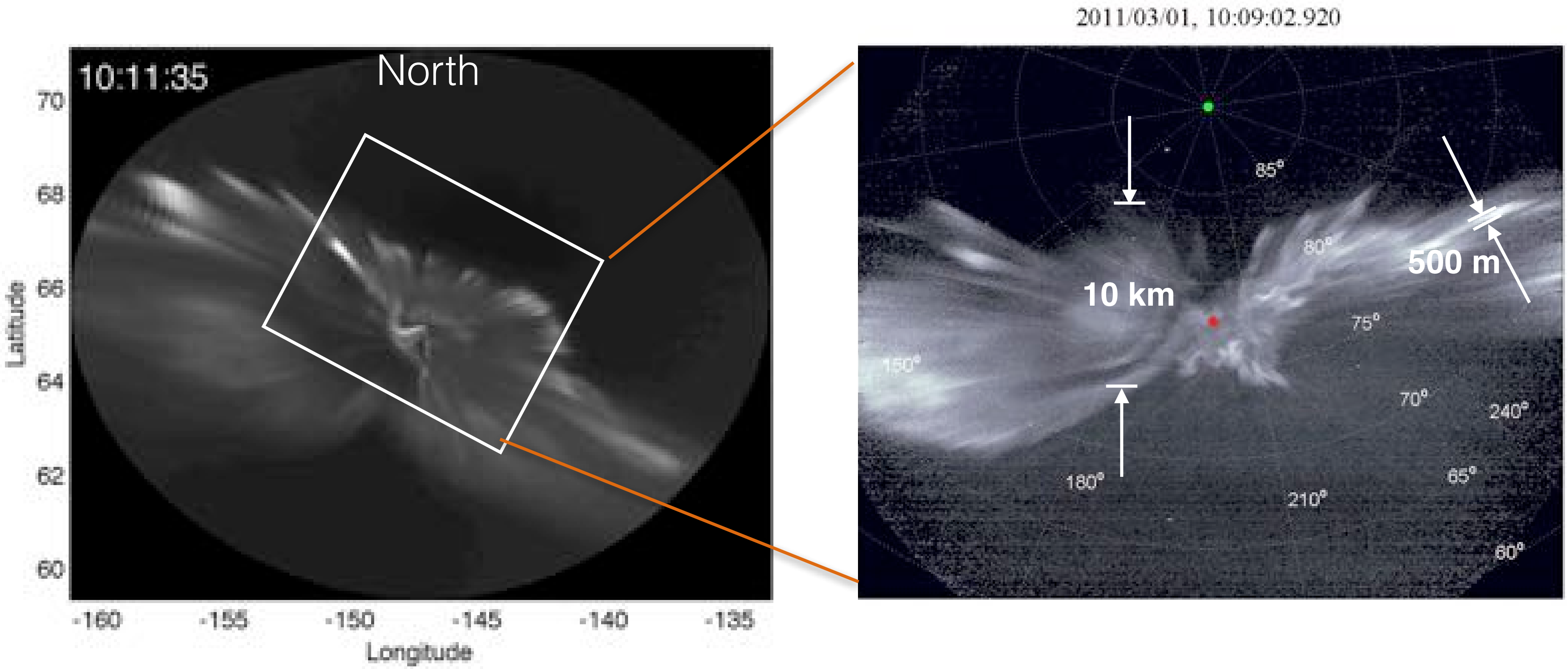

Optical manifestation of dispersive bursts

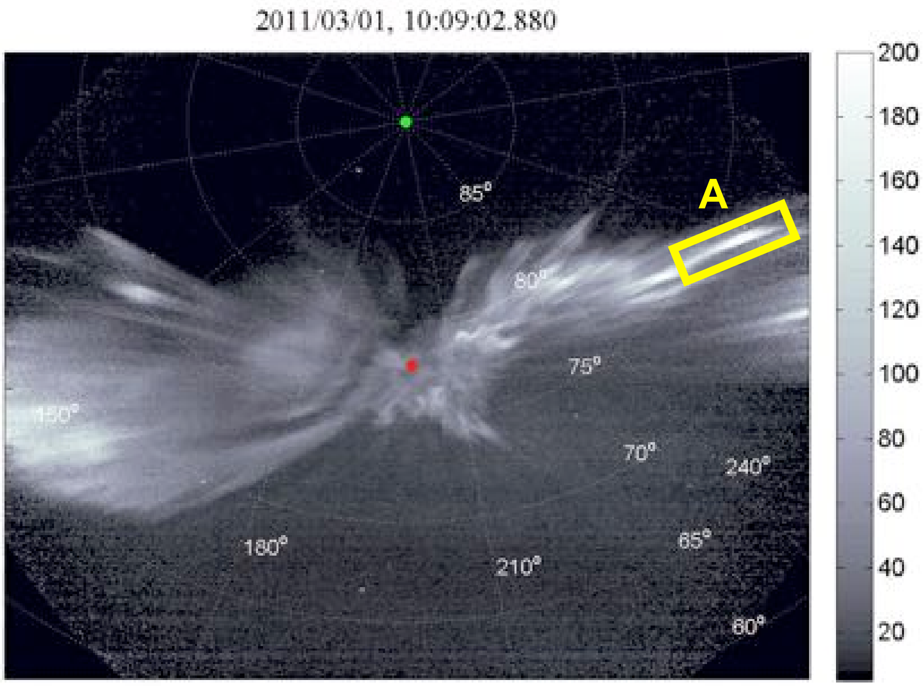

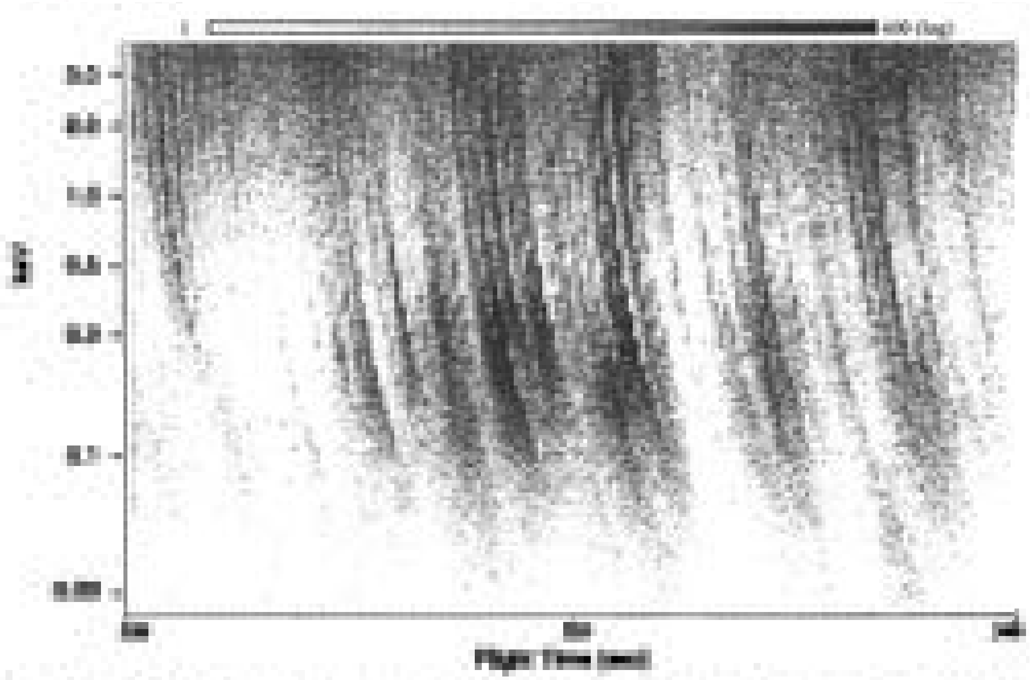

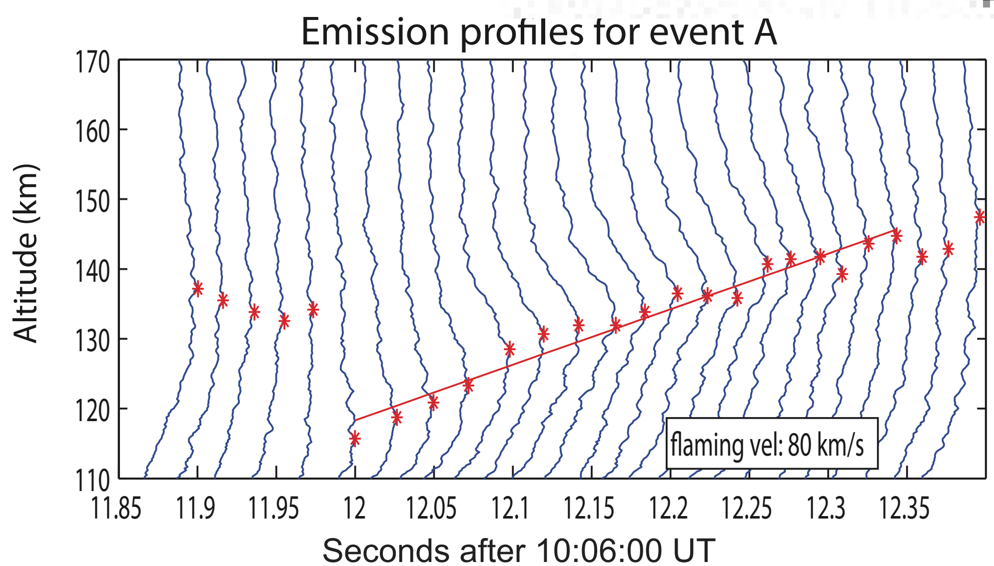

Average energy of primary electrons decreases
from 3keV to <500eV in 0.2-s.

Dahlgren et al., JGRA 2013.

Alfven waves

MHD (dispersionless)

$$\omega = k_z v_A$$

$$v_A = \frac{B_o}{\sqrt{\mu_o \rho}}$$

With Inertial Correction

$$\omega^2 = \frac{k_\parallel^2 v_A^2}{1 + k_\perp^2 \lambda_e^2}$$

$$\frac{\partial \omega}{\partial \mathbf{k}} = \hat{\mathbf{z}} \frac{v_A}{(1 + k_\perp^2 \lambda_e^2)^{1/2}} - \hat{\mathbf{x}} \omega \lambda_e \frac{k_\perp \lambda_e}{1 + k_\perp^2 \lambda_e^2}$$

A backward wave!

$$m_e \frac{\partial u_{e\parallel}}{\partial t} = q_e E_\parallel$$

$$J_\parallel = n q_e u_{e\parallel}$$

$$\lambda_e = \frac{c}{\omega_{pe}}$$

$$\omega_{pe}^2 = \frac{n_0 q^2}{m_e \epsilon_o}$$

Combine, take F.T.

$$\boxed{\tilde{E}_\parallel = i \omega \lambda_e^2 \mu_o \tilde{J}_\parallel}$$

Aurora

Semeter et al., JGRA 2009.